Delft University of Technology

Consensus in high-power multiagent systems with mixed unknown control directions via hybrid Nussbaum-based control

Lv, Maolong; Yu, Wenwu; Cao, Jinde; Baldi, Simone

DOI
10.1109/TCYB.2020.3028171

Publication date
2020

Document Version
Accepted author manuscript

Published in
IEEE Transactions on Cybernetics

Citation (APA)
Lv, M., Yu, W., Cao, J., & Baldi, S. (2020). Consensus in high-power multiagent systems with mixed unknown control directions via hybrid Nussbaum-based control. *IEEE Transactions on Cybernetics*, *52 (2022)*(6), 5184-5196. https://doi.org/10.1109/TCYB.2020.3028171

Consensus in High-Power Multiagent Systems With Mixed Unknown Control Directions via Hybrid Nussbaum-Based Control

Maolong Lv, Wenwu Yu, *Senior Member, IEEE*, Jinde Cao, *Fellow, IEEE*, and Simone Baldi, *Senior Member, IEEE*

***Abstract*—This work investigates the consensus tracking problem for high-power nonlinear multiagent systems with partially unknown control directions. The main challenge of considering such dynamics lies in the fact that their linearized dynamics contain uncontrollable modes, making the standard backstepping technique fail; also, the presence of mixed unknown control directions (some being known and some being unknown) requires a piecewise Nussbaum function that exploits the *a priori* knowledge of the known control directions. The piecewise Nussbaum function technique leaves some open problems, such as Can the technique handle multiagent dynamics beyond the standard backstepping procedure? and Can the technique handle more than one control direction for each agent? In this work, we propose a hybrid Nussbaum technique that can handle uncertain agents with high-power dynamics where the backstepping procedure fails, with nonsmooth behaviors (switching and quantization), and with multiple unknown control directions for each agent.**

***Index Terms*—Consensus tracking, input quantization, multiagent systems, switched dynamics, unknown control directions.**

I. Introduction

During the last two decades, the coordination of multiagent systems has gained tremendous attention, where the consensus problem is one of the most studied coordination tasks [1]–[3]. Consensus problems have been studied for various classes of uncertain and nonlinear agent dynamics, including multiagent systems with unparameterized nonlinearities [4]–[9]; switched multiagent systems [10]–[12]; nonsmooth multiagent systems (e.g., with quantization, saturation, deadzone, etc.) [11], [13]; multiagent systems with unknown control directions [13]–[15]; time-delay multiagent systems [9], [16]; event-triggered multiagent systems [17], [18]; and so on. Most of these approaches to consensus rely on a distributed version of the well-known backstepping iterative procedure [19]. Such a procedure, also known in the literature as adding-one-linear-integrator procedure, introduces one linear integrator at each iteration and can be applied to strict-feedback [4]–[9], [20]–[22] and pure-feedback multiagent systems [10]–[12], [23], [24]. The procedure can be successfully combined with tools known for single-agent systems, such as function approximators [25]–[29], switched Lyapunov functions [30]–[33], and so on. However, for some classes of nonlinear systems, the adding-one-linear-integrator backstepping procedure cannot be applied. The most famous example is the high-power dynamics, also known in the literature as high-order nonlinear dynamics: for this class, the adding-one-power-integrator procedure was proposed in [34] by introducing iteratively one high-power integrator instead of a linear one. The procedure was further extended in a distributed sense, and combined with function approximators and switched Lyapunov function [35], [36]. The class of high-power dynamics is the object of the present work, which we study via the Nussbaum function method in the presence of multiple unknown control directions and nonsmooth behaviors (switching and quantization).

The Nussbaum function method to handle unknown control directions [37]–[41] has not been explored in the distributed adding-one-power-integrator scenario, that is, for coordination of multiagent systems with high-power dynamics. The peculiar characteristic of a Nussbaum function lies in its capability of alternatively changing sign. This characteristic will occasionally provide inputs in the "wrong" direction, leading to large transients [37], [42], [43]. The transient issue becomes even more pronounced in networks with unknown control directions. The Nussbaum function method is challenging even for multiagent systems controlled with the distributed adding-one-linear-integrator backstepping procedure [44]–[46]: researchers have studied unknown but identical control directions [44], mixed unknown control directions

Manuscript received February 19, 2020; revised July 12, 2020; accepted September 18, 2020. This work was supported in part by the Natural Science Foundation of China under Grant 61833005, Grant 61673107, and Grant 62073076; and in part by the Special Guiding Funds Double First-Class under Grant 3307012001A. This article was recommended by Associate Editor A. Gasparri. *(Corresponding author: Simone Baldi.)*

Maolong Lv is with School of Control Science and Engineering, Air Force Engineering University, Xi'an 710051, China, and also with the Delft Center for Systems and Control, Delft University of Technology, 2628 CD Delft, The Netherlands (e-mail: m.lyu@tudelft.nl).

Wenwu Yu is with the School of Mathematics, Southeast University, Nanjing 210096, China (e-mail: jdcao@seu.edu.cn).

Jinde Cao is with the School of Mathematics, Southeast University, Nanjing 210096, China, and also with the Yonsei Frontier Laboratory, Yonsei University, Seoul 03722, South Korea (e-mail: jdcao@seu.edu.cn).

Simone Baldi is with the School of Mathematics, Southeast University, Nanjing 210096, China, and also with the Delft Center for Systems and Control, Delft University of Technology, 2628 CD Delft, The Netherlands (e-mail: s.baldi@tudelft.nl).

Color versions of one or more of the figures in this article are available online at http://ieeexplore.ieee.org.

Digital Object Identifier 10.1109/TCYB.2020.3028171

(some directions being known and some being unknown) via a piecewise Nussbaum function that exploits the *a priori* knowledge of the known control directions [45], [46] or multiple nonidentical unknown control directions with switching topologies [14], [15] and communication delays [16].

For the single-agent case, it was shown that addressing multiple unknown control directions requires novel conditional inequalities involving the summation of multiple Nussbaum functions terms [39]; a novel Nussbaum function whose sign keeps the same on some periods of time was proposed in [41], so that the Nussbaum integral terms do not cancel each other in the summation. Recently, the properties of different classes of Nussbaum functions, namely, type A and type B have been investigated for handling constant and time-varying unknown control coefficients [42], [43]. Even when a single control direction is considered for each agent [44]–[46], a summation of Nussbaum terms occurs as the result of considering a global conditional inequality for the whole network. Therefore, the Nussbaum function should be carefully designed to avoid cancelation of the integral terms. The aforementioned investigations open the questions on whether techniques exist to handle high-power dynamics (for which adding-one-linear-integrator backstepping would fail) in the presence of multiple unknown control directions. The main contribution of this work is to give positive answers to these questions.

1) To the best of our knowledge, this is the first Nussbaum-based approach going beyond the distributed adding-one-linear-integrator backstepping setting, by considering uncertain agents with high-power dynamics.
2) The Nussbaum function techniques in [37]–[41] are designed to handle one unknown control direction for each agent, whereas the proposed technique uses hybrid Nussbaum gains that can handle multiple mixed unknown directions for each agent.
3) The proposed technique can handle nonsmooth behavior, that is, switching dynamics and input quantization. The relevance of considering input quantization stems from works, such as [47] and [48], showing that appropriate designs must be proposed in the presence of input nonlinearities. Our proposed design relies on a variable-separable lemma to extract quantized control signal in a "linear-like" manner.

The remainder of this article is organized as follows. Preliminaries and problem formulation are given in Section II. Sections III and IV present the proposed distributed protocol and stability analysis, respectively. The simulation results are in Section V and Section VI draws the conclusions.

II. Preliminaries and Problem Formulation

A. Graph Theory

A weighted directed graph describes how agents interact with each other: the agents are represented by nodes, and the interactions by edges. A weighted directed graph is defined by $\mathcal{G} = (\mathcal{V}, \mathcal{E}, \mathcal{A})$, with the node set being $\mathcal{V} = \{v_1, \dots, v_N\}$ ($N \geq 2$), the edge set being $\mathcal{E} \subseteq \mathcal{V} \times \mathcal{V}$, and the adjacency matrix $\mathcal{A} = [a_{fl}] \in \mathbb{R}^{N\times N}$ being utilized to represent the communication topology among the agents. An edge $e_{fl} = (f, l) \in \mathcal{E}$ means that agent l can receive information from agent f. The set of nodes to which an agent f can send information is denoted by $\mathcal{N}_f$, representing the neighboring set. The entries $a_{f,l}$ of the adjacency matrix $\mathcal{A}$ are defined as follows: if the information of agent l can be received by agent f, $a_{fl} > 0$; otherwise, $a_{fl} = 0$. Let us also define the diagonal matrix $\mathcal{D} = \mathrm{diag}[d_1, \dots, d_N] \in \mathbb{R}^{N\times N}$ with $d_f = \sum_{l=1}^{N} a_{fl}$. The Laplacian matrix of $\mathcal{G}$ is defined as $\mathcal{L} = \mathcal{D} - \mathcal{A}$. The communication topology for the N follower agents and a leader agent is defined as an augmented directed graph $\bar{\mathcal{G}} = (\bar{\mathcal{V}}, \bar{\mathcal{E}})$ with $\bar{\mathcal{V}} = \{v_0, v_1, \dots, v_N\}$ and $\bar{\mathcal{E}} \subseteq \bar{\mathcal{V}} \times \bar{\mathcal{V}}$ where index 0 is used for the leader agent. The set of neighbors of the fth follower agent in $\bar{\mathcal{G}}$ is denoted as $\bar{\mathcal{N}}_f$. Then, the Laplacian matrix $\bar{\mathcal{L}}$ corresponding to $\bar{\mathcal{G}}$ is defined as

$$\bar{\mathcal{L}} = \begin{bmatrix} 0 & \mathbf{0}_{N\times 1}^T \\ -b & \mathcal{H} \end{bmatrix}$$

where $\mathbf{0}_{N\times 1} = [0, \dots, 0]^T \in \mathbb{R}^{N\times 1}$, $\mathcal{H} = \mathcal{L} + \mathcal{B}$, $\mathcal{L}$ is the Laplacian matrix of the subgraph $\mathcal{G}$, and $\mathcal{B}$ is the leader agent adjacency matrix defined as $\mathcal{B} = \mathrm{diag}[b_1, \dots, b_N]$ where $b_i > 0$ if $0 \in \bar{\mathcal{N}}_f, f = 1, \dots, N$, and $b_i = 0$ otherwise, and $b = [b_1, \dots, b_N]^T$. The directed graph $\bar{\mathcal{G}}$ is said to have a spanning tree with the root node being the leader if a directed path exists from the leader to all the other nodes.

Assumption 1 [49]: The graph $\bar{\mathcal{G}}$ contains a spanning tree with the root node being the leader. This implies that $\bar{\mathcal{L}} + \mathcal{B}$ is a nonsingular $\mathcal{M}$-matrix.

B. Problem Statement

Let us consider a multiagent system composed of $N (N \geq 2)$ follower agents, under a directed communication topology described by $\mathcal{G} = (\mathcal{V}, \mathcal{E}, \mathcal{A})$. Let the dynamics of the fth follower agent, $f = 1, \dots, N$, be represented by the high-power nonlinear dynamics

$$\begin{cases} \dot{\chi}_{f,m} = \varphi_{f,m}^{\sigma_f(t)}\left(\bar{\chi}_{f,m}\right) + \phi_{f,m}^{\sigma_f(t)}\left(\bar{\chi}_{f,m}\right)\chi_{f,m+1}^{r_{f,m}} \\ \dot{\chi}_{f,n_f} = \varphi_{f,n_f}^{\sigma_f(t)}\left(\chi_f\right) + \phi_{f,n_f}^{\sigma_f(t)}\left(\chi_f\right)\left(Q_f\left(u_f\right)\right)^{r_{f,n_f}} \\ y_f \quad = \chi_{f,1} \end{cases} \tag{1}$$

where $1 \leq m \leq n_f - 1$, $\bar{\chi}_{f,m} = [\chi_{f,1}, \chi_{f,2}, \dots, \chi_{f,m}]^T \in \mathbb{R}^m$, $\chi_f = [\chi_{f,1}, \chi_{f,2}, \dots, \chi_{f,n_f}]^T \in \mathbb{R}^{n_f}$, and $y_f \in \mathbb{R}$ are the states and the output of the fth follower agent, respectively. For $f = 1, \dots, N$ and $m = 1, \dots, n_f$, $\varphi_{f,m}^{\sigma_f(t)}(\cdot)$ and $\phi_{f,m}^{\sigma_f(t)}(\cdot)$ are unknown continuous nonlinearities, and $r_{f,m}$ are positive odd integers. In (1), $\sigma_f(\cdot) : [0, +\infty) \to \mathcal{M}_f = \{1, 2, \dots, m_f\}$ is a switching signal which selects at each time t the nonlinearities for agent f among m_f possibilities. The control signal to be designed is u_f, with the quantized input $Q_f(u_f)$ being defined as

$$Q_f(u_f) = \begin{cases} u_{f,h}\mathrm{sgn}(u_f), & \text{if} \begin{cases} \frac{u_{f,h}}{1+\hbar_f} < |u_f| \leq u_{f,h}, \dot{u}_f < 0, \text{ or} \\ u_{f,h} < |u_f| \leq \frac{u_{f,h}}{1-\hbar_f}, \dot{u}_f > 0, \end{cases} \\ \bar{u}_{f,h}\mathrm{sgn}(u_f), & \text{if} \begin{cases} u_{f,h} < |u_f| \leq \frac{u_{f,h}}{1-\hbar_f}, \dot{u}_f < 0, \text{ or} \\ \frac{u_{f,h}}{1-\hbar_f} < |u_f| \leq \frac{u_{f,h}(1+\hbar_f)}{1-\hbar_f}, \dot{u}_f > 0, \end{cases} \\ 0, & \text{if} \begin{cases} 0 \leq |u_f| \leq \frac{u_f^{\min}}{1+\hbar_f}, \dot{u}_f < 0, \text{ or} \\ \frac{u_f^{\min}}{1+\hbar_f} < |u_f| \leq u_f^{\min}, \dot{u}_f > 0, \end{cases} \\ Q_f(u_f(t^-)), & \text{otherwise} \end{cases} \tag{2}$$

with $\bar{u}_{f,h} = u_{f,h}(1+\hbar_f)$, $u_{f,h} = \rho_f^{1-h} u_f^{\min}(h = 1, 2, \ldots)$ and $\hbar_f = [(1-\rho_f)/(1+\rho_f)]$ with $u_f^{\min} > 0$ and $0 < \rho_f < 1$, and $u_f^{\min}$ and ρ_f represent the deadzone range of $Q_f(u_f)$ and the measure of quantization density, respectively. Due to quantization, we have that the continuous signal u_f is mapped into a discrete set $\mathscr{F}_f = \{0, \pm u_{f,h}, \pm u_{f,h}(1+\hbar_f), h = 1, 2, \ldots\}$.

Remark 1: The quantizer parameter ρ_f, $f = 1, \ldots, N$, is a measure of quantization density. The smaller ρ_f, the coarser the quantizer, that is, $Q_f(u_f)$ will have less and less quantization levels [47], [48].

Lemma 1 [47]: The relation between the continuous input u_f and the quantized input $Q_f(u_f)$ can be described by

$$Q_f(u_f) = \kappa_f(u_f)u_f + \Delta_f(u_f) \tag{3}$$

where $\kappa_f(u_f)$ and $\Delta_f(u_f)$ satisfy $1 - \hbar_f \le \kappa_f(u_f) \le 1 + \hbar_f$, and $|\Delta_f(u_f)| \le u_f^{\min}$.

Remark 2: When all the powers $r_{f,m}$ are equal to one, the multiagent dynamics in [44]–[46] are obtained. However, a different design is required because, while the dynamics in [44]–[46] allow the use of the adding-one-linear-integrator procedure (backstepping), this procedure cannot be used for (1) (see discussion in [34]).

The leader agent 0 is represented by a leader output signal $y_L(\cdot)$. As compared to a single-agent case, the challenge of controlling multiple agents is that not all the agents can access the leader signal.

Assumption 2 [49]: The leader output signal $y_L(\cdot)$ is continuous, bounded, and available only to a subset of the follower agents according to the graph $\bar{\mathcal{G}}$. Furthermore, $\dot{y}_L(\cdot)$ is bounded and not available to any follower agent. The bounds for $y_L(\cdot)$ and $\dot{y}_L(\cdot)$ are unknown.

Assumption 3 [35]: For each follower agent f, there exist known constants $\underline{\phi}_{f,m} > 0$ and $\bar{\phi}_{f,m} > 0$, $(1 \le m \le n_f)$ such that

$$\underline{\phi}_{f,m} \le \left|\phi_{f,m}^k(\cdot)\right| \le \bar{\phi}_{f,m}, \quad k \in \mathcal{M}_f.$$

Furthermore, some control directions of $\phi_{f,m}$ can be unknown.

Remark 3: Assumption 2 implies that the leader output is continuously differentiable, which is standard in [49]. The bounds $\underline{\phi}_{f,m}$ and $\overline{\phi}_{f,m}$ ensure the controllability of each agent, but instead of assuming known sign of $\phi_{f,m}^k$ as in [35], [36], and [50], Assumption 3 allows some signs to be unknown.

Problem 1: The goal is consensus tracking, that is, to design u_f such that the output of each agent can track the leader agent's signal while respecting the communication topology defined by the graph $\bar{\mathcal{G}}$. Practical consensus tracking will be sought, due to the fact that asymptotic tracking cannot be realized in general for high-power systems [51].

It is worth mentioning that the problem of unknown control directions for the dynamics (1) is open and requires a new design that is not available in the literature.

C. Nussbaum-Based Technical Tools

In this section, we give the main result concerning hybrid Nussbaum-based control. To counteract the lack of *a priori* knowledge of control directions, we define the Nussbaum function as [45]

$$\mathcal{N}_R(\nu) = \begin{cases} \mathcal{N}_R^{\bar{1}}(\nu), & \text{if unknown control direction} \\ \mathcal{N}_R^{\bar{2}}(\nu), & \text{if known control direction} \end{cases} \tag{4}$$

where $N_R^{\bar{1}}(\nu) = -\mu \exp(\nu^2/2)(\nu^2+2)\sin(\nu)$, and $N_R^{\bar{2}}(\nu) = -\exp(\nu^2/2)\nu$ with ν being a real variable and μ being a positive constant.

Remark 4: To explain the meaning of (4), note that in the mixed situation in which some control directions are known and some are unknown, it is not appropriate to adopt the standard Nussbaum function for every agent. This is because, differently from the hybrid Nussbaum function in (4), a standard Nussbaum function typically does not guarantee a boundedness of the summation of multiple Nussbaum integral terms [39], [41].

The following result is proposed to establish the boundedness of a Lyapunov function when a hybrid Nussbaum function as in (4) is adopted.

Lemma 2: Let $V_f(t)$ be a smooth positive-definite function with bounded initial value $V_f(0)$. Let $\xi_{f,n}(t)$ for $n = 1, 2, \ldots, n_f$ be smooth and increasing functions with their initial values $\xi_{f,n}(0)$ bounded. Furthermore, let $\phi_{f,n}(t)$ be a time-varying gain, nonzero in the closed interval $[\underline{\phi}_{f,n}, \bar{\phi}_{f,n}]$ for $f = 1, 2, \ldots, N$. If the following inequality holds:

$$\begin{aligned} V_f(t) \le \sum_{n=1}^{n_f} \int_0^t \phi_{f,n}(\nu)\theta_{f,n}\mathcal{N}_R\big(\xi_{f,n}(\nu)\big)\dot{\xi}_{f,n}(\nu) \\ + \sum_{n=1}^{n_f} \int_0^t \iota_f \dot{\xi}_{f,n}(\nu)d\nu + \varpi_f \end{aligned} \tag{5}$$

where ι_f and ϖ_f are constants, $\theta_{f,n}$ is a positive and bounded function, and $\mathcal{N}_R(\cdot)$ as in (4), then $\xi_{f,n}(t)$, $V_f(t)$, and $\sum_{n=1}^{n_f} \int_0^t (\phi_{f,n}(\nu)\theta_{f,n}\mathcal{N}_R(\xi_{f,n}(\nu)) + \iota_f)\dot{\xi}_{f,n}(\nu)d\nu$ are bounded on the time interval $[0, t_\nu)$ for $f = 1, 2, \ldots, N$.

Proof: See Appendix A. ■

Remark 3: Similar to the lemmas in [12], [13], [16], [29], and [44]–[46], the proposed lemma (Lemma 2) holds over a finite-time interval. Such lemmas to the entire time domain are not trivial, as discussed in [52]. Nevertheless, works such as [16] have shown that boundedness on the entire time domain can be obtained during stability analysis, by using the continuation of the maximal solution of the closed-loop system. In this work, we will adopt a similar argument to obtain stability (see proof of Theorem 1).

D. Other Technical Tools and Lemmas

The following technical lemmas will be employed to derive the main results of this article.

Lemma 3 [50]: Let $x_1, x_2 \in \mathbb{R}$ be real-valued functions. There exist a positive odd integer b and a constant $\bar{\lambda} \ge 1$ such that

$$\left|x_1^b - x_2^b\right| \le b|x_1 - x_2|\left|x_1^{b-1} + x_2^{b-1}\right|$$
$$|x_1 + x_2|^{\bar{\lambda}} \le 2^{\bar{\lambda}-1}\left(|x_1|^{\bar{\lambda}} + |x_2|^{\bar{\lambda}}\right).$$

Lemma 4 [50]: Let $x_1, x_2 \in \mathbb{R}$ and r_1 and r_2 be positive constants. For any real-valued function $\upsilon(\cdot,\cdot) > 0$, one has

$$|x_1|^{r_1}|x_2|^{r_2} \le \frac{r_1}{r_1+r_2}\upsilon|x_1|^{r_1+r_2} + \frac{r_2}{r_1+r_2}\upsilon^{-\frac{r_1}{r_2}}|x_2|^{r_1+r_2}.$$

Lemma 5 [11]: For any $x_1, x_2 \in \mathbb{R}$ and positive odd integer b, there exist real-valued functions $\zeta_1(\cdot,\cdot)$ and $\zeta_2(\cdot,\cdot)$ such that

$$(x_1+x_2)^b = \zeta_1(x_1,x_2)x_1^b + \zeta_2(x_1,x_2)x_2^b$$

where $\zeta_1(x_1,x_2) \in [1-\bar{\epsilon}, 1+\bar{\epsilon}]$ for $\forall\bar{\epsilon} \in (0,1)$ and $|\zeta_2(x_1,x_2)| \le M$ where M is a positive constant that is independent of x_1 and x_2.

Lemma 6 [25]: For any continuous function $h(Z)$ defined on a compact set Ω_Z, for $\forall\bar{\varepsilon} > 0$, there exists a fuzzy-logic system (FLS) $y(Z) = W^{*T}\Xi(Z)$ such that

$$\sup_{Z\in\Omega_Z}\left|h(Z) - W^{*T}\Xi(Z)\right| \le \bar{\varepsilon} \tag{6}$$

where W^* is the ideal parameter vector, and $\Xi(Z)$ is the fuzzy basic function vector.

III. Proposed Consensus Tracking Design

To start the design, let us define $r_f = \max_{1\le m\le n_f}\{r_{f,m}\}$ and let us define the following changes of coordinates:

$$\begin{cases} e_{f,1} = \sum_{l\in\bar{\mathcal{N}}_f} a_{fl}(y_f - y_l) + b_f(y_f - y_L) \\ e_{f,m} = \chi_{f,m} - \alpha_{f,m}, \quad m = 2,3,\ldots,n_f \end{cases} \tag{7}$$

where $\alpha_{f,m}$ represents the virtual control law which will be specified later. After defining $e_1 = [e_{1,1}, e_{2,1}, \ldots, e_{N,1}]^T \in \mathbb{R}^N$, one has $e_1 = (\bar{\mathcal{L}} + \mathcal{B})\delta$ where $\delta = \bar{y} - \bar{y}_L$ with $\bar{y} = [y_1, y_2, \ldots\ldots, y_N]^T$ and $\bar{y}_L = [y_L, y_L, \ldots, y_L]^T$. Due to the nonsingularity of $\bar{\mathcal{L}} + \mathcal{B}$, it holds that $\|\delta\| \le \frac{\|e_1\|}{\underline{\sigma}(\bar{\mathcal{L}}+\mathcal{B})}$, being $\underline{\sigma}(\bar{\mathcal{L}} + \mathcal{B})$ the minimum singular value of $\bar{\mathcal{L}} + \mathcal{B}$.

The design proceeds iteratively along with the following steps.

Step 1 for the fth Agent ($f \in \{1,\ldots,N\}$): Using (1) and (7), we obtain the time derivative of $e_{f,1}$ as

$$\dot{e}_{f,1} = (d_f + b_f)\phi_{f,1}^k(\chi_{f,1})\chi_{f,2}^{r_{f,1}} + H_{f,1}^k(Z_{f,1}), \ \ k \in \mathcal{M}_f \tag{8}$$

where $Z_{f,1} = [\chi_{f,1}, \chi_{l,1}, \chi_{l,2}]^T (l \in \bar{\mathcal{N}}_f)$ and

$$H_{f,1}^k(Z_{f,1}) = -\sum_{l\in\bar{\mathcal{N}}_f} a_{fl}\left(\phi_{l,1}^k(\chi_{l,1})\chi_{l,2}^{r_{l,1}} + \varphi_{l,1}^k(\chi_{l,1})\right) + (d_f+b_f)\varphi_{f,1}^k(\chi_{l,1}) - b_f\dot{y}_L. \tag{9}$$

From Lemma 6, it follows that the unknown continuous function $H_{f,1}^k(Z_{f,1})$ can be approximated by

$$H_{f,1}^k(Z_{f,1}) = W_{f,1}^{k*T}\Xi_{f,1}^k(Z_{f,1}) + \varepsilon_{f,1}^k(Z_{f,1})$$

where $|\varepsilon_{f,1}^k(Z_{f,1})| \le \bar{\varepsilon}_{f,1}^k$ includes both the bounded approximation error and the bounded $\dot{y}_L$.

According to Lemma 4, it holds that

$$\begin{aligned} &e_{f,1}^{r_f-r_{f,1}+3}H_{f,1}^k \\ &\le \frac{r_f - r_{f,1}+3}{r_f+3}\nu_{f,1}^{\frac{r_f+3}{r_f-r_{f,1}+3}} e_{f,1}^{r_f+3}\left\|W_{f,1}^{k*}\right\|^{\frac{r_f+3}{r_f-r_{f,1}+3}}\left\|\Xi_{f,1}^k\right\|^{\frac{r_f+3}{r_f-r_{f,1}+3}} \\ &\quad + \frac{r_{f,1}}{r_f+3}\varsigma_{f,1}^{-\frac{r_f+3}{r_{f,1}}}\bar{\varepsilon}_{f,1}^{k\frac{r_f+3}{r_{f,1}}} + \frac{r_{f,1}}{r_f+3}\ell_{f,1}^{-\frac{r_f+3}{r_{f,1}}} \\ &\quad + \frac{r_f - r_{f,1}+3}{r_f+3}\varsigma_{f,1}^{\frac{r_f+3}{r_f-r_{f,1}+3}}e_{f,1}^{r_f+3} \\ &\le e_{f,1}^{r_f+3}\left(\ell_{f,1}^{\frac{r_f+3}{r_f-r_{f,1}+3}}\beta_{f,1}\left\|\Xi_{f,1}\right\|^{\frac{r_f+3}{r_f-r_{f,1}+3}} + \varsigma_{f,1}^{\frac{r_f+3}{r_f-r_{f,1}+3}}\right) + \lambda_{f,1} \end{aligned} \tag{10}$$

where $\beta_{f,1} = \max\{\beta_{f,1}^k, k \in \mathcal{M}_f\}$, $\Xi_{f,1} = \max\{\Xi_{f,1}^k, k \in \mathcal{M}_f\}$, $\beta_{f,1}^k = \|W_{f,1}^{k*}\|^{([r_f+3]/[r_f-r_{f,1}+3])}$, $\bar{\varepsilon}_{f,1} = \max\{\bar{\varepsilon}_{f,1}^k, k \in \mathcal{M}_f\}$, and $\lambda_{f,1} = \ell_{f,1}^{-([r_f+3]/[r_{f,1}])} + \varsigma_{f,1}^{-([r_f+3]/[r_{f,1}])}\bar{\varepsilon}_{f,1}^{([r_f+3]/[r_{f,1}])}$.

Let us start constructing the Lyapunov function as

$$V_{f,1} = \frac{e_{f,1}^{r_f-r_{f,1}+4}}{r_f - r_{f,1}+4} + \frac{1}{2\vartheta_{f,1}}\tilde{\beta}_{f,1}^2 \tag{11}$$

where $\tilde{\beta}_{f,1} = \beta_{f,1} - \hat{\beta}_{f,1}$ and $\vartheta_{f,1} > 0$ is a design parameter.

It follows from (8), (10), and (11) that the time derivative of $V_{f,1}$ is:

$$\begin{aligned} \dot{V}_{f,1} &\le e_{f,1}^{r_f-r_{f,1}+3}(d_f+b_f)\left(\phi_{f,1}^k(\chi_{f,1})\alpha_{f,2}^{r_{f,1}} + e_{f,1}^{r_{f,1}}\psi_{f,1}\right) \\ &\quad - \frac{\tilde{\beta}_{f,1}\dot{\hat{\beta}}_{f,1}}{\vartheta_{f,1}} + e_{f,1}^{r_f+3}\ell_{f,1}^{\frac{r_f+1}{r_f-r_{f,1}+3}}\beta_{f,1}\left\|\Xi_{f,1}\right\|^{\frac{r_f+3}{r_f-r_{f,1}+3}} \\ &\quad + e_{f,1}^{r_f-r_{f,1}+3}(d_f+b_f)\phi_{f,1}^k(\chi_{f,1})\left(\chi_{f,2}^{r_{f,1}} - \alpha_{f,2}^{r_{f,1}}\right) \\ &\quad - e_{f,1}^{r_f+3}(d_f+b_f)\psi_{f,1} + e_{f,1}^{r_f+3}\varsigma_{f,1}^{\frac{r_f+3}{r_f-r_{f,1}+3}} + \lambda_{f,1}. \end{aligned} \tag{12}$$

Design the virtual controllers $\alpha_{f,2}$ and adaptive laws $\hat{\beta}_{f,1}$ as

$$\alpha_{f,2} = \mathcal{N}_R^{\frac{1}{r_{f,1}}}(\xi_{f,1})\psi_{f,1}^{\frac{1}{r_{f,1}}}e_{f,1} \tag{13}$$

$$\psi_{f,1} = (d_f+b_f)^{-1}\left(\ell_{f,1}^{\frac{r_f+3}{r_f-r_{f,1}+3}}\hat{\beta}_{f,1}\left\|\Xi_{f,1}\right\|^{\frac{r_f+3}{r_f-r_{f,1}+3}} + c_{f,1} + \varsigma_{f,1}^{\frac{r_f+3}{r_f-r_{f,1}+3}}\right) \tag{14}$$

$$\dot{\xi}_{f,1} = e_{f,1}^{r_f+3}(d_f+b_f)\psi_{f,1} \tag{15}$$

$$\dot{\hat{\beta}}_{f,1} = \vartheta_{f,1}\ell_{f,1}^{\frac{r_f+3}{r_f-r_{f,1}+3}}e_{f,1}^{r_f+3}\left\|\Xi_{f,1}\right\|^{\frac{r_f+3}{r_f-r_{f,1}+3}} - \gamma_{f,1}\hat{\beta}_{f,1} \tag{16}$$

where $\ell_{f,1}$, $c_{f,1}$, $\gamma_{f,1}$, and $\varsigma_{f,1}$ are positive design parameters.

Substituting (13)–(16) into (12) yields

$$\begin{aligned} \dot{V}_{f,1} &\le e_{f,1}^{r_f-r_{f,1}+3}(d_f+b_f)\phi_{f,1}(\chi_{f,1})\left(\chi_{f,2}^{r_{f,1}} - \alpha_{f,2}^{r_{f,1}}\right) \\ &\quad + \dot{\xi}_{f,1}\left(\phi_{f,1}(\chi_{f,1})\mathcal{N}_R(\xi_{f,1}) + 1\right) + \lambda_{f,1} \\ &\quad + \frac{1}{\vartheta_{f,1}}\gamma_{f,1}\tilde{\beta}_{f,1}\hat{\beta}_{f,1} - c_{f,1}e_{f,1}^{r_f+3}. \end{aligned} \tag{17}$$

By using Lemmas 3 and 4, we have that

$$\begin{aligned} &\left|e_{f,1}^{r_f-r_{f,1}+3}\phi_{f,1}(\chi_{f,1})\left(\chi_{f,2}^{r_{f,1}} - \alpha_{f,2}^{r_{f,1}}\right)\right| \\ &\le \frac{\eta_{f,1}^{-r_f}e_{f,2}^{r_f+3}}{r_f+3}\left(r_{f,1}\bar{\phi}_{f,1}\mathcal{N}_R^{\frac{1}{r_{f,1}}}(\xi_{f,1})\psi_{f,1}^{\frac{r_{f,1}-1}{r_{f,1}}}\right)^{r_f+3} \end{aligned}$$

$$
\begin{aligned}
&+ \frac{r_{f,1} e_{f,2}^{r_f+3}}{r_f+3} \eta_{f,1}^{-\frac{r_f - r_{f,1}+3}{r_{f,1}}} \left(2^{r_{f,1}-2} r_{f,1} \bar{\phi}_{f,1}\right)^{\frac{r_f+3}{r_{f,1}}} \\
&+ \frac{\eta_{f,1}^{-r_f} e_{f,2}^{r_f+3}}{r_f+3} \left(2^{r_{f,1}-2} r_{f,1} \bar{\phi}_{f,1} \psi_{f,1}^{r_{f,1}-1}\right)^{r_f+3} \\
&+ \frac{r_f - r_{f,1}+7}{r_f+3} \eta_{f,1} e_{f,1}^{r_f+1} + \frac{2 r_f \eta_{f,1} e_{f,1}^{r_f+1}}{r_f+3} \\
\le\ & e_{f,1}^{r_f+3} + \left(d_f + b_f\right)^{-1} e_{f,2}^{r_f+3} \Theta_{f,1} \qquad (18)
\end{aligned}
$$

with $\eta_{f,1} = ([r_f+3]/[3r_f - r_{f,1}+7])$ and $\Theta_{f,1}$ being a function given by

$$
\begin{aligned}
\Theta_{f,1} = \left(d_f + b_f\right) \Bigg[& \frac{r_{f,1}}{r_f+3} \eta_{f,1}^{-\frac{r_f - r_{f,1}+3}{r_{f,1}}} \left(2^{r_{f,1}-2} r_{f,1} \bar{\phi}_{f,1}\right)^{\frac{r_f+3}{r_{f,1}}} \\
&+ \frac{1}{r_f+3} \eta_{f,1}^{-r_f} \left(r_{f,1} \bar{\phi}_{f,1} \mathcal{N}_R^{\frac{1}{r_{f,1}}}(\xi_{f,1}) \psi_{f,1}^{\frac{r_{f,1}-1}{r_{f,1}}} \right)^{r_f+3} \\
&+ \frac{1}{r_f+3} \eta_{f,1}^{-r_f} \left(2^{r_{f,1}-2} r_{f,1} \bar{\phi}_{f,1} \psi_{f,1}^{r_{f,1}-1}\right)^{r_f+3} \Bigg].
\end{aligned}
$$

From (18), the time derivative of $V_{f,1}$ can be rewritten as

$$
\begin{aligned}
\dot{V}_{f,1} \le\ & \frac{\gamma_{f,1}}{\vartheta_{f,1}} \tilde{\beta}_{f,1} \hat{\beta}_{f,1} - \left(c_{f,1} - \left(d_f + b_f\right)\right) e_{f,1}^{r_f+3} \\
&+ \dot{\xi}_{f,1}\left(\phi_{f,1}\left(\chi_{f,1}\right) \mathcal{N}_R\left(\xi_{f,1}\right) + 1\right) \\
&+ e_{f,2}^{r_f+3} \Theta_{f,1} + \lambda_{f,1}. \qquad (19)
\end{aligned}
$$

Defining $\phi_{f,1} = \max\{\phi_{f,1}^k, k \in \mathcal{M}_f\}$ and using Young's inequality

$$
\tilde{\beta}_{f,1} \hat{\beta}_{f,1} = \left(\tilde{\beta}_{f,1} \beta_{f,1} - \tilde{\beta}_{f,1}^2\right) \le \frac{1}{2}\left(\beta_{f,1}^2 - \tilde{\beta}_{f,1}^2\right) \qquad (20)
$$

it can be obtained that $\dot{V}_{f,1}$ is

$$
\begin{aligned}
\dot{V}_{f,1} \le\ & \dot{\xi}_{f,1}\left(\phi_{f,1}(\chi_{f,1}) \mathcal{N}_R(\xi_{f,1}) + 1\right) + e_{f,2}^{r_f+3} \Theta_{f,1} \\
&- \left(c_{f,1} - (d_f + b_f)\right) e_{f,1}^{r_f+3} + \lambda_{f,1} \\
&+ \frac{\gamma_{f,1}}{2\vartheta_{f,1}} \left(\beta_{f,1}^2 - \tilde{\beta}_{f,1}^2\right). \qquad (21)
\end{aligned}
$$

Step m for the fth Agent ($f \in \{1, \ldots, N\}$, $m \in \{2, \ldots, n_f - 1\}$): From (1) and (7), the time derivative of $e_{f,m}$ is given by

$$
\dot{e}_{f,m} = \phi_{f,m}^k\left(\bar{\chi}_{f,m}\right) \chi_{f,m+1}^{r_{f,m}} + H_{f,m}^k\left(Z_{f,m}\right), \ \ k \in \mathcal{M}_f \qquad (22)
$$

where $Z_{f,m} = [\bar{\chi}_{f,m}^T, \bar{\chi}_{l,m}^T, \bar{\hat{\beta}}_{f,m-1}, \bar{\xi}_{f,m-1}, y_L]^T (l \in \bar{\mathcal{N}_f})$, $\bar{\hat{\beta}}_{f,m-1} = [\hat{\beta}_{f,1}, \hat{\beta}_{f,2}, \ldots, \hat{\beta}_{f,m-1}]$, $\bar{\xi}_{f,m-1} = [\xi_{f,1}, \xi_{f,2}, \ldots, \xi_{f,m-1}]$ and

$$
\begin{aligned}
& H_{f,m}^k\left(Z_{f,m}\right) = \\
& \quad - \sum_{n=1}^{m-1} \sum_{l \in \bar{\mathcal{N}_f}} \frac{\partial \alpha_{f,m}}{\partial \chi_{l,n}} \left(\phi_{l,n}^k\left(\bar{\chi}_{l,n}\right) \chi_{l,n+1}^{r_{l,n}} + \varphi_{l,n}^k\left(\bar{\chi}_{l,n}\right)\right) \\
& \quad - \sum_{n=1}^{m-1} \frac{\partial \alpha_{f,m}}{\partial \chi_{f,n}} \left(\phi_{f,n}^k\left(\bar{\chi}_{f,n}\right) \chi_{f,n+1}^{r_{f,n}} + \varphi_{f,n}^k\left(\bar{\chi}_{f,n}\right)\right) \\
& \quad - \frac{\partial \alpha_{f,m}}{\partial y_L} \dot{y}_L - \sum_{n=1}^{m-1} \frac{\partial \alpha_{f,m}}{\partial \hat{\beta}_{f,n}} \dot{\hat{\beta}}_{f,n} \\
& \quad - \sum_{n=1}^{m-1} \frac{\partial \alpha_{f,m}}{\partial \xi_{f,n}} \dot{\xi}_{f,n} + \varphi_{f,m}^k(\bar{\chi}_{f,m}). \qquad (23)
\end{aligned}
$$

Along similar lines as step 1, the following inequality holds:

$$
\begin{aligned}
e_{f,m}^{r_f - r_{f,m}+3} H_{f,m}^k\left(Z_{f,m}\right) \le\ & e_{f,m}^{r_f+3} \varsigma_{f,m}^{\frac{r_f+3}{r_f - r_{f,m}+3}} + \lambda_{f,m} \\
&+ e_{f,m}^{r_f+3} \ell_{f,m}^{\frac{r_f+3}{r_f - r_{f,m}+3}} \beta_{f,m} \left\| \Xi_{f,m} \right\|^{\frac{r_f+3}{r_f - r_{f,m}+3}} \qquad (24)
\end{aligned}
$$

where $\beta_{f,m}^k = \|W_{f,m}^{k*}\|^{([r_f+3]/[r_f - r_{f,m}+3])}$, $\beta_{f,m} = \max\{\beta_{f,m}^k, k \in \mathcal{M}_f\}$, $\Xi_{f,m} = \max\{\Xi_{f,m}^k, k \in \mathcal{M}_f\}$, $\bar{\varepsilon}_{f,m} = \max\{\bar{\varepsilon}_{f,m}^k, k \in \mathcal{M}_f\}$, and $\lambda_{f,m} = \ell_{f,m}^{-([(r_f+3)]/[r_{f,m}])} + \varsigma_{f,m}^{-([(r_f+3)]/[r_{f,m}])} \bar{\varepsilon}_{f,m}^{([(r_f+3)]/[r_{f,m}])}$.

Starting from (11), the Lyapunov function is constructed iteratively as

$$
V_{f,m} = V_{f,m-1} + \frac{e_{f,m}^{r_f - r_{f,m}+4}}{r_f - r_{f,m}+4} + \frac{1}{2\vartheta_{f,m}} \tilde{\beta}_{f,m}^2 \qquad (25)
$$

where $\tilde{\beta}_{f,m} = \beta_{f,m} - \hat{\beta}_{f,m}$ and $\vartheta_{f,m} > 0$ is a design constant.

Combining (21), (22), and (24) with (25), the time derivative of $V_{f,m}$ is written as

$$
\begin{aligned}
\dot{V}_{f,m} \le\ & e_{f,m}^{r_f+3} \Theta_{f,m-1} - e_{f,m}^{r_f - r_{f,m}+3} \phi_{f,m}^k\left(\bar{\chi}_{f,m}\right) \alpha_{f,m+1}^{r_{f,m}} \\
&+ e_{f,m}^{r_f - r_{f,m}+3} \phi_{f,m}\left(\bar{\chi}_{f,m}\right) \left(\chi_{f,m+1}^{r_{f,m}} - \alpha_{f,m+1}^{r_{f,m}}\right) \\
&+ \sum_{n=1}^{m-1} \left(\frac{\gamma_{f,n}}{2\vartheta_{f,n}} \left(\beta_{f,n}^2 - \tilde{\beta}_{f,n}^2\right)\right) - \frac{\tilde{\beta}_{f,m} \dot{\hat{\beta}}_{f,m}}{\vartheta_{f,m}} \\
&- \sum_{n=2}^{m-1} \left(c_{f,n} - 1\right) e_{f,n}^{r_f+3} + e_{f,m}^{r_f+3} \varsigma_{f,m}^{\frac{r_f+3}{r_f - r_{f,m}+3}} \\
&+ e_{f,m}^{r_f+3} \ell_{f,m}^{\frac{r_f+3}{r_f - r_{f,m}+3}} \beta_{f,m} \| \Xi_{f,m} \|^{\frac{r_f+3}{r_f - r_{f,m}+3}} \\
&+ \sum_{n=1}^{m-1} \dot{\xi}_{f,n}\left(\phi_{f,n}\left(\bar{\chi}_{f,n}\right) \mathcal{N}_R\left(\xi_{f,n}\right) + 1\right) \\
&+ \sum_{n=1}^{m} \lambda_{f,n} - \left(c_{f,1} - \left(d_f + b_f\right)\right) e_{f,1}^{r_f+3}. \qquad (26)
\end{aligned}
$$

Design the virtual controllers $\alpha_{f,m+1}$ and adaptive laws $\hat{\beta}_{f,m}$ as

$$
\alpha_{f,m+1} = \mathcal{N}_R^{\frac{1}{r_{f,m}}}\left(\xi_{f,m}\right) e_{f,m} \psi_{f,m}^{\frac{1}{r_{f,m}}} \qquad (27)
$$

$$
\begin{aligned}
\psi_{f,m} = c_{f,m} + \ell_{f,m}^{\frac{r_f+3}{r_f - r_{f,m}+3}} \hat{\beta}_{f,m} \left\| \Xi_{f,m} \right\|^{\frac{r_f+3}{r_f - r_{f,m}+3}} + \Theta_{f,m-1} \\
+ \varsigma_{f,m}^{\frac{r_f+3}{r_f - r_{f,m}+3}} \qquad (28)
\end{aligned}
$$

$$
\dot{\xi}_{f,m} = e_{f,m}^{r_f+3} \psi_{f,m} \qquad (29)
$$

$$
\dot{\hat{\beta}}_{f,m} = \vartheta_{f,m} \ell_{f,m}^{\frac{r_f+3}{r_f - r_{f,m}+3}} e_{f,m}^{r_f+3} \left\| \Xi_{f,m} \right\|^{\frac{r_f+3}{r_f - r_{f,m}+3}} - \gamma_{f,m} \hat{\beta}_{f,m} \qquad (30)
$$

where $\ell_{f,m}, c_{f,m}, \gamma_{f,m}$, and $\varsigma_{f,m}$ are positive design parameters.

Substituting (27)–(30) into (26) and along similar lines as (17)–(20), we can obtain the time derivative of $V_{f,m}$ as

$$
\begin{aligned}
\dot{V}_{f,m} \le\ & e_{f,m+1}^{r_f+3} \Theta_{f,m} - \left(c_{f,1} - \left(d_f + b_f\right)\right) e_{f,1}^{r_f+3} \\
&+ \sum_{n=1}^{m} \dot{\xi}_{f,n}\left(\phi_{f,n}\left(\bar{\chi}_{f,n}\right) \mathcal{N}_R\left(\xi_{f,n}\right) + 1\right)
\end{aligned}
$$

$$+\sum_{n=1}^{m}\lambda_{f,n}-\sum_{n=2}^{m}\left(c_{f,n}-1\right)e_{f,n}^{r_f+3}$$
$$+\sum_{n=1}^{m}\left(\frac{\gamma_{f,n}}{2\vartheta_{f,n}}\left(\beta_{f,n}^2-\tilde{\beta}_{f,n}^2\right)\right) \tag{31}$$

where $\phi_{f,m}=\max\left\{\phi_{f,m}^k, k\in\mathcal{M}_f\right\}$.

Step n_f for the fth agent ($f\in\{1,\ldots,N\}$): In view of Lemma 5 and using (1), (3), and (7), the time derivative of e_{f,n_f} can be written as

$$\dot{e}_{f,n_f}\leq\phi_{f,n_f}^k\left(\chi_f\right)\zeta_{1,f}\kappa_f^{r_{f,n_f}}u_f^{r_{f,n_f}}+H_{f,n_f}^k\left(Z_{f,n_f}\right),\ k\in\mathcal{M}_f \tag{32}$$

where $Z_{f,n_f}=\left[\chi_f^T,\chi_l^T,\bar{\hat{\beta}}_{f,n_f-1},\bar{\xi}_{f,n_f-1},y_L\right]^T(l\in\bar{\mathcal{N}}_f)$, $\bar{\hat{\beta}}_{f,n_f-1}=\left[\hat{\beta}_{f,1},\hat{\beta}_{f,2},\ldots,\hat{\beta}_{f,n_f-1}\right]$, $\bar{\xi}_{f,n_f-1}=\left[\xi_{f,1},\xi_{f,2},\ldots,\xi_{f,n_f-1}\right]$ and

$$\begin{aligned}&H_{f,n_f}^k\left(Z_{f,n_f}\right)=\\&\quad-\sum_{n=1}^{n_f-1}\sum_{l\in\bar{\mathcal{N}}_f}\frac{\partial\alpha_{f,n_f}}{\partial\chi_{l,n}}\left(\phi_{l,n}^k\left(\bar{\chi}_{l,n}\right)\chi_{l,n+1}^{r_{l,n}}+\varphi_{l,n}^k\left(\chi_l\right)\right)\\&\quad-\sum_{n=1}^{n_f-1}\frac{\partial\alpha_{f,n_f}}{\partial\chi_{f,n}}\left(\phi_{f,n}^k\left(\bar{\chi}_{f,n}\right)\chi_{f,n+1}^{r_{f,n}}+\varphi_{f,n}^k\left(\chi_f\right)\right)\\&\quad-\sum_{n=1}^{n_f-1}\frac{\partial\alpha_{f,n_f}}{\partial\hat{\beta}_{f,n}}\dot{\hat{\beta}}_{f,n}-\frac{\partial\alpha_{f,m}}{\partial y_L}\dot{y}_L+\varphi_{f,n_f}^k\left(\chi_f\right)\\&\quad-\sum_{n=1}^{n_f-1}\frac{\partial\alpha_{f,n_f}}{\partial\xi_{f,n}}\dot{\xi}_{f,n}+\phi_{f,n_f}^k\left(\chi_f\right)\zeta_{2,f}\Delta_f(t)^{r_{f,n_f}}.\end{aligned} \tag{33}$$

Similar to step f,m, it can be obtained that

$$\begin{aligned}e_{f,n_f}^{r_f-r_{f,n_f}+3}H_{f,n_f}^k\left(Z_{f,n_f}\right)&\leq e_{f,n_f}^{r_f+3}\varsigma_{f,n_f}^{\frac{r_f+3}{r_f-r_{f,n_f}+3}}+\lambda_{f,n_f}\\&\quad+e_{f,n_f}^{r_f+3}\ell_{f,n_f}^{\frac{r_f+3}{r_f-r_{f,n_f}+3}}\beta_{f,n_f}\|\Xi_{f,n_f}\|^{\frac{r_f+3}{r_f-r_{f,n_f}+3}}\end{aligned} \tag{34}$$

where $\beta_{f,n_f}^k=\left\|W_{f,n_f}^{k*}\right\|^{([r_f+3]/[r_f-r_{f,n_f}+3])}$, $\beta_{f,n_f}=\max\left\{\beta_{f,n_f}^k, k\in\mathcal{M}_f\right\}$, $\Xi_{f,n_f}=\max\left\{\Xi_{f,n_f}^k, k\in\mathcal{M}_f\right\}$, $\bar{\varepsilon}_{f,n_f}=\max\left\{\bar{\varepsilon}_{f,n_f}^k, k\in\mathcal{M}_f\right\}$ and $\lambda_{f,n_f}=\ell_{f,n_f}^{-([r_f+3]/[r_{f,n_f}])}+\varsigma_{f,n_f}^{-([r_f+3]/[r_{f,n_f}])}\bar{\varepsilon}_{f,n_f}^{([r_f+3]/[r_{f,n_f}])}$.

The last step in the construction of the Lyapunov function for agent f is

$$V_{f,n_f}=V_{f,n_f-1}+\frac{e_{f,n_f}^{r_f-r_{f,n_f}+4}}{r_f-r_{f,n_f}+4}+\frac{1}{2\vartheta_{f,n_f}}\tilde{\beta}_{f,n_f}^2 \tag{35}$$

where $\tilde{\beta}_{f,n_f}=\beta_{f,n_f}-\hat{\beta}_{f,n_f}$ and $\vartheta_{f,n_f}>0$ is a design parameter.

The derivative of V_{f,n_f} along (31), (32), and (34) is given by

$$\begin{aligned}\dot{V}_{f,n_f}&\leq\sum_{n=1}^{n_f}\lambda_{f,n}+\sum_{n=1}^{n_f-1}\dot{\xi}_{f,n}\left(\phi_{f,n}\left(\bar{\chi}_{f,n}\right)\mathcal{N}_R\left(\xi_{f,n}\right)+1\right)\\&\quad-\sum_{n=2}^{n_f-1}\left(c_{f,n}-1\right)e_{f,n}^{r_f+3}-\left(c_{f,1}-\left(d_f+b_f\right)\right)e_{f,1}^{r_f+3}\\&\quad+\sum_{n=1}^{n_f-1}\left(\frac{\gamma_{f,n}}{2\vartheta_{f,n}}\left(\beta_{f,n}^2-\tilde{\beta}_{f,n}^2\right)\right)-\frac{\tilde{\beta}_{f,n_f}\dot{\hat{\beta}}_{f,n_f}}{\vartheta_{f,n_f}}\\&\quad+e_{f,n_f}^{r_f+3}\ell_{f,n_f}^{\frac{r_f+3}{r_f-r_{f,n_f}+3}}\beta_{f,n_f}\|\Xi_{f,n_f}\|^{\frac{r_f+3}{r_f-r_{f,n_f}+3}}\\&\quad+e_{f,n_f}^{r_f-r_{f,n_f}+3}\phi_{f,n_f}^k\left(\chi_f\right)\zeta_{1,f}\kappa_f^{r_{f,n_f}}u_f^{r_{f,n_f}}\\&\quad+e_{f,n_f}^{r_f+3}\varsigma_{f,n_f}^{\frac{r_f+3}{r_f-r_{f,n_f}+3}}+\Theta_{f,n_f-1}e_{f,n_f}^{r_f+3}.\end{aligned} \tag{36}$$

Let us design the actual controller u_f and parameters adaption laws $\hat{\beta}_{f,n_f}$ as follows:

$$u_f=\mathcal{N}_R^{\frac{1}{r_{f,n_f}}}\left(\xi_{f,n_f}\right)\psi_{f,n_f}^{\frac{1}{r_{f,n_f}}}e_{f,n_f} \tag{37}$$

$$\begin{aligned}\psi_{f,n_f}&=c_{f,n_f}+\ell_{f,n_f}^{\frac{r_f+3}{r_f-r_{f,n_f}+3}}\hat{\beta}_{f,n_f}\|\Xi_{f,n_f}\|^{\frac{r_f+3}{r_f-r_{f,n_f}+3}}\\&\quad+\Theta_{f,n_f-1}+\varsigma_{f,n_f}^{\frac{r_f+3}{r_f-r_{f,n_f}+3}}\end{aligned} \tag{38}$$

$$\dot{\xi}_{f,n_f}=e_{f,n_f}^{r_f+3}\psi_{f,n_f} \tag{39}$$

$$\begin{aligned}\dot{\hat{\beta}}_{f,n_f}&=\vartheta_{f,n_f}\ell_{f,n_f}^{\frac{r_f+3}{r_f-r_{f,n_f}+3}}e_{f,n_f}^{r_f+3}\|\Xi_{f,n_f}\|^{\frac{r_f+3}{r_f-r_{f,n_f}+3}}\\&\quad-\gamma_{f,n_f}\hat{\beta}_{f,n_f}\end{aligned} \tag{40}$$

where ℓ_{f,n_f}, c_{f,n_f}, λ_{f,n_f}, and ς_{f,n_f} are positive design parameters.

Substituting (37)–(40) into (36) results in

$$\begin{aligned}\dot{V}_{f,n_f}&\leq\sum_{n=1}^{n_f}\lambda_{f,n}+\sum_{n=1}^{n_f}\frac{\gamma_{f,n}}{2\vartheta_{f,n}}\beta_{f,n}^2-\sum_{n=2}^{n_f}\left(c_{f,n}-1\right)e_{f,n}^{r_f+3}\\&\quad-\sum_{n=1}^{n_f}\frac{\gamma_{f,n}}{2\vartheta_{f,n}}\tilde{\beta}_{f,n}^2-\left(c_{f,1}-\left(d_f+b_f\right)\right)e_{f,1}^{r_f+3}\\&\quad+\sum_{n=1}^{n_f}\dot{\xi}_{f,n}\left(\phi_{f,n}\left(\bar{\chi}_{f,n}\right)\theta_{f,n}\mathcal{N}_R\left(\xi_{f,n}\right)+1\right)\end{aligned} \tag{41}$$

where $\phi_{f,n_f}=\max\left\{\phi_{f,n_f}^k, k\in\mathcal{M}_f\right\}$, and when $1\leq n\leq n_f-1$, let $\theta_{f,n}=1$, when $n=n_f$, let $\theta_{f,n}=\zeta_{1,f}\kappa_f^{r_{f,n_f}}$.

IV. Stability Analysis

We are now at the position to present the main results of the proposed method in the following theorem.

Theorem 1: Under Assumptions 1–3, consider the closed-loop multiagent system composed by the high-power switched nonlinear dynamics (1), the virtual control laws (13) and (27), the actual control law (37), and the parameter adaptation laws (14)–(16), (28)–(30), and (38)–(40). Then, it holds that: 1) all signals of the closed-loop multiagent system remain bounded and 2) the tracking error δ converges to the compact set Ω_e defined by

$$\Omega_e=\left\{\|\delta\|\leq\sqrt{\frac{N^{N-1}\left(N^2+N-1\right)^2\sum_{f=1}^{N}\Upsilon_f^2}{(N-1)^{N-1}}}\right\}$$

where $\Upsilon_f = \left(\left(\Pi_f + P_f\right)\left(r_f - r_{f,1} + 4\right)\right)^{(1/[r_f - r_{f,1}+4])}$. The constants Π_f and P_f are not given here for compactness, but they are derived during the proof.

Proof: See Appendix B. ■

Remark 4: Consensus tracking is solved in Theorem 1 via a common Lyapunov function, by estimating the maximum value of the switching weights in the linear-in-the-parameter approximator [see (10), (24), and (34)]. A multiple Lyapunov function approach is in principle possible by estimating different switching weights for different subsystems. However, in this case, the stability analysis becomes more challenging because it requires to impose conditions at switching instants, whereas a common Lyapunov function can guarantee stability under arbitrary switching.

Remark 5: Some guidelines for selecting appropriate design parameters are: 1) choosing small positive constants $\gamma_{f,m}$ and increasing $\vartheta_{f,m}$ results in a faster convergence rate of adaptation parameters $\widehat{\beta}_{f,m}$; 2) decreasing $c_{f,m}$, $\lambda_{f,m}$, and $\gamma_{f,m}$, while increasing $\vartheta_{f,m}$ helps to reduce ϱ_f, and thus reduces the size of Ω_e; and 3) enhancing the connectivity of the communication link $\bar{\mathcal{L}} + \mathcal{B}$ also contributes to reduce the size of Ω_e.

Remark 6: To clarify the importance of Lemma 2 and Theorem 1, consider that [39] has shown that the summation of conditional inequality may be bounded even when each term approaches infinity individually, but with opposite signs. For example, to avoid this problem, Huang *et al.* [41] proposed new Nussbaum functions having the same signs on some periods of time. The results in [45] and [46] proposed conditional inequalities where no sign assumption is necessary; however, these results are applied to systems with one single control direction. Lemma 2 and Theorem 1 solved the open problem of handling multiple mixed unknown control directions with multiple hybrid Nussbaum functions.

V. Simulation Results

In this section, we provide one numerical and one practical examples to validate the effectiveness of the proposed scheme.

A. Numerical Example

One leader (labeled by 0) with three (switched) follower agents is considered by the directed graph as in Fig. 1.

From Fig. 1, it can be seen that the signal of leader is accessible to follower 1 only. The leader output is $y_L(t) = 5\sin(t) + 10\sin(0.5t)$. The follower agents are described by the following dynamics:

$$\begin{cases} \dot{\chi}_{1,1} = \varphi_{1,1}^{\sigma_f(t)}(\chi_{1,1}) + \phi_{1,1}^{\sigma_f(t)}(\chi_{1,1})\chi_{1,2}^3 \\ \dot{\chi}_{1,2} = \varphi_{1,2}^{\sigma_f(t)}(\chi_1) + \phi_{1,2}^{\sigma_f(t)}(\chi_1)(Q_1(u_1))^3 \\ \dot{\chi}_{2,1} = \varphi_{2,1}^{\sigma_f(t)}(\chi_{2,1}) + \phi_{2,1}^{\sigma_f(t)}(\chi_{2,1})\chi_{2,2}^3 \\ \dot{\chi}_{2,2} = \varphi_{2,2}^{\sigma_f(t)}(\chi_2) + \phi_{2,2}^{\sigma_f(t)}(\chi_2)(Q_2(u_2))^5 \\ \dot{\chi}_{3,1} = \varphi_{3,1}^{\sigma_f(t)}(\chi_{3,1}) + \phi_{3,1}^{\sigma_f(t)}(\chi_{3,1})\chi_{3,2}^5 \\ \dot{\chi}_{3,2} = \varphi_{3,2}^{\sigma_f(t)}(\chi_3) + \phi_{3,2}^{\sigma_f(t)}(\chi_3)(Q_3(u_3))^5 \\ y_f = \chi_{f,1}, f = 1,2,3 \end{cases} \tag{42}$$

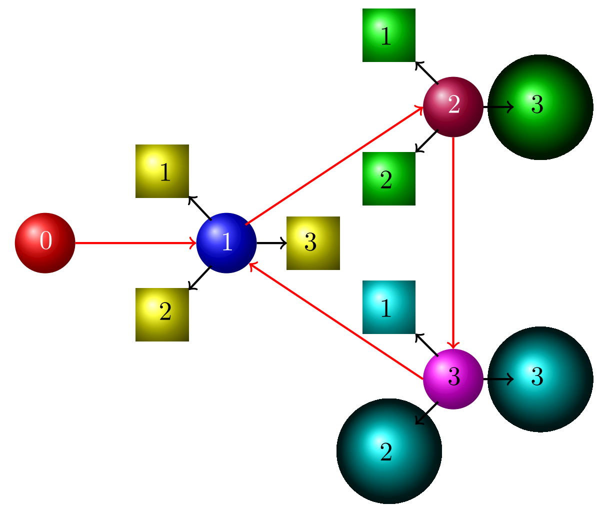

Fig. 1. Communication graph between leader 0 and follower agents 1–3. Each agent can switch among three dynamics, represented as three squares around each agent.

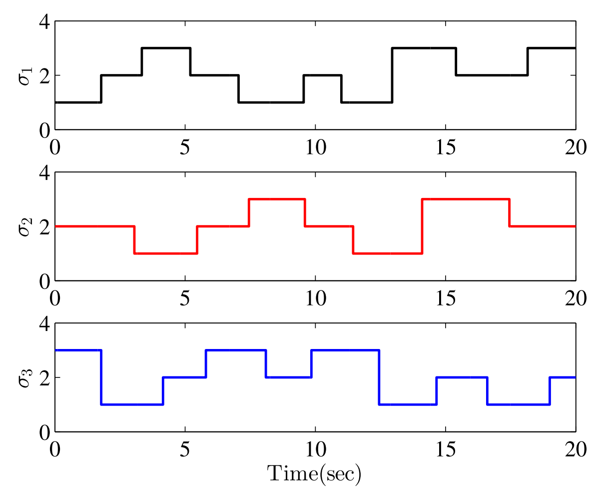

Fig. 2. Asynchronous switching signals $\sigma_f(t)$.

where $\sigma_f(\cdot)$: $[0, +\infty) \to \mathcal{M}_f = \{1,2,3\}$: note that each follower has its own switching signal, and thus can switch asynchronously with respect to the other followers (see Fig. 2).

For follower agent 1, the three switching dynamics are

$$\begin{aligned} &\varphi_{1,1}^1 = 1.3 - \cos(\chi_{1,1}), && \phi_{1,1}^1 = \left|\tanh\left(\chi_{1,2}^3\right)\right| + 1.6 \\ &\varphi_{1,1}^2 = 0.6 + \exp\left(-\chi_{1,2}^2\right), && \phi_{1,1}^2 = \cos\left(\chi_{1,1}^3\right) + 2 \\ &\varphi_{1,1}^3 = 0.8 + 0.2\cos(\chi_{1,1}), && \phi_{1,1}^3 = 2\cos(\chi_{1,2})^2 \\ &\varphi_{1,2}^1 = \chi_{1,2}\chi_{1,1} + 0.8, && \phi_{1,2}^1 = 2\left(\left|\cos\left(\chi_{1,1}^2\right)\right| + 1.3\right) \\ &\varphi_{1,2}^2 = 0.7 + 0.2\chi_{1,2}^2, && \phi_{1,2}^2 = 3\sin(\chi_{1,2})^2 + 4 \\ &\varphi_{1,2}^3 = \cos\left(\chi_{1,2}^2\right) + 0.3, && \phi_{1,2}^3 = 5|\sin(0.1\chi_{1,1})| + 1.5. \end{aligned}$$

For follower agent 2, the three switching dynamics are

$$\begin{aligned} &\varphi_{2,1}^1 = 1.1\chi_{2,1} + \chi_{2,2}, && \phi_{2,1}^1 = 1.5\sin\left(\chi_{2,1}^2 + \chi_{2,2}^2\right) \\ &\varphi_{2,1}^2 = \chi_{2,1}^2\chi_{2,2}, && \phi_{2,1}^2 = \sin\left(\chi_{2,2}\chi_{2,1}^2\right) + 2.5 \end{aligned}$$

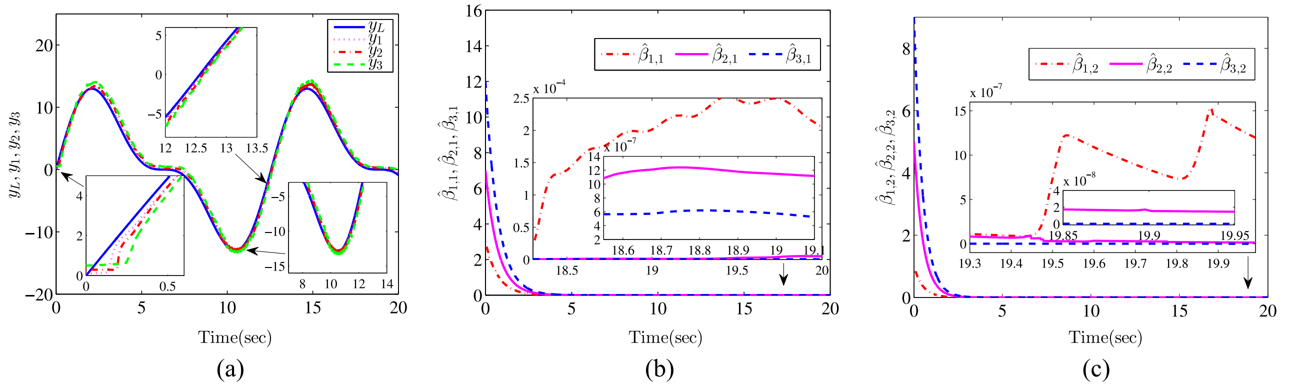

Fig. 3. Evolutions of (a) y_L, y_1, y_2, and y_3, (b) $\widehat{\beta}_{1,1}$, $\widehat{\beta}_{2,1}$, and $\widehat{\beta}_{3,1}$, and (c) $\widehat{\beta}_{1,2}$, $\widehat{\beta}_{2,2}$, and $\widehat{\beta}_{3,2}$.

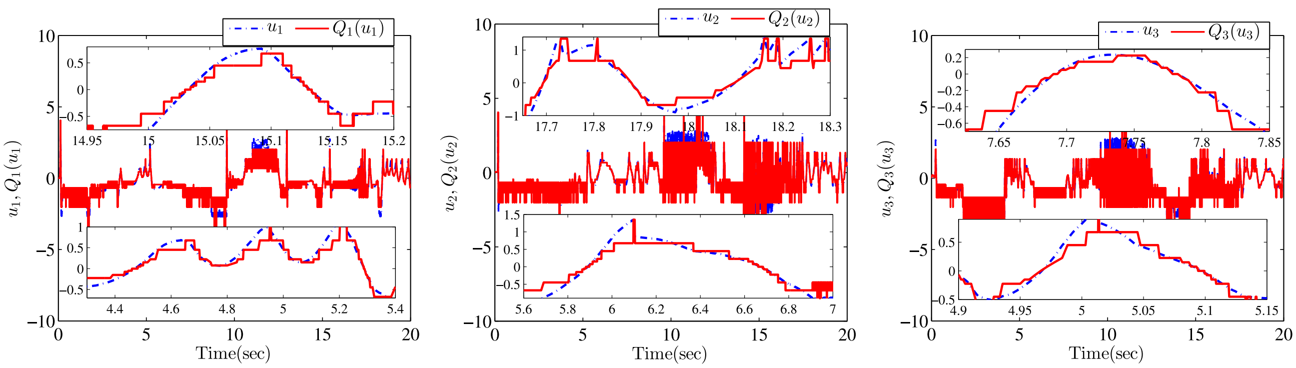

Fig. 4. Trajectories of u_1 and $Q_1(u_1)$, u_2 and $Q_2(u_2)$, and u_3 and $Q_3(u_3)$.

$$\varphi_{2,1}^3 = \chi_{2,1}\chi_{2,2}^2 + 1.2, \quad \phi_{2,1}^3 = \cos\left(\chi_{2,2}^2\chi_{2,1}^3\right) + 3$$
$$\varphi_{2,2}^1 = \chi_{2,1}\chi_{2,2}^2 + 0.5, \quad \phi_{2,2}^1 = 3 + 2\cos\left(\chi_{2,1}^3\chi_{2,2}\right)$$
$$\varphi_{2,2}^2 = 1.3\chi_{2,2}^3 + 0.8\chi_{2,1}, \quad \phi_{2,2}^2 = 2\cos\left(\chi_{2,1}^2\right) + 4$$
$$\varphi_{2,2}^3 = \cos(\chi_{2,1})\chi_{2,2}, \quad \phi_{2,2}^3 = 5 + 3\sin\left(\chi_{2,2}\chi_{2,1}^2\right).$$

For follower agent 3, the three switching dynamics are

$$\varphi_{3,1}^1 = 1.5\sin(\chi_{3,2}) + \chi_{3,1}, \quad \phi_{3,1}^1 = |\sin(\chi_{3,1})| + 6$$
$$\varphi_{3,1}^2 = 0.3\chi_{3,1}^2 + \sin(\chi_{3,2}), \quad \phi_{3,1}^2 = \left|\sin\left(\chi_{3,2}^3\right)\right| + 3$$
$$\varphi_{3,1}^3 = \chi_{3,1} + 0.2\chi_{3,2}, \quad \phi_{3,1}^3 = \cos\left(\chi_{3,2}^2\chi_{3,1}^3\right) + 4.5$$
$$\varphi_{3,2}^1 = 0.5\chi_{3,1}^2 + \chi_{3,2}, \quad \phi_{3,2}^1 = \cos\left(\chi_{3,2}^2\right) + 2$$
$$\varphi_{3,2}^2 = \chi_{3,2} + 0.8\sin(\chi_{3,1}), \quad \phi_{3,2}^2 = 4\cos(\chi_{3,1}) + 5.5$$
$$\varphi_{3,2}^3 = \cos(\chi_{3,2})^2 + 0.7, \quad \phi_{3,2}^3 = \cos(\chi_{3,2})^3 + 3.5.$$

While conducting the simulation, the control directions of $\phi_{f,1}^{\sigma_f}$, $\sigma_f = 1, 2, 3, f = 1, 2, 3$, are assumed known and the control directions of $\phi_{f,2}^{\sigma_f}$, $\sigma_f = 1, 2, 3$, $f = 1, 2, 3$, are assumed unknown. The initial conditions are $\chi_1(0) = [0.1, -0.1]^T$, $\chi_2(0) = [0.3, -0.3]^T$, $\chi_3(0) = [0.5, -0.5]^T$, $\hat{\beta}_{1,1}(0) = 3$, $\hat{\beta}_{1,2}(0) = 1$, $\hat{\beta}_{2,1}(0) = 7$, $\hat{\beta}_{2,2}(0) = 5$, $\hat{\beta}_{3,1}(0) = 12$, $\hat{\beta}_{3,2}(0) = 9$, and $\xi_{1,1}(0) = \xi_{1,2}(0) = \xi_{2,1}(0) = \xi_{2,2}(0) = \xi_{3,1}(0) = \xi_{3,2}(0) = 0$. The design parameters are chosen to be $c_{1,1} = c_{2,1} = c_{3,1} = 10$, $c_{1,2} = c_{2,2} = c_{3,2} = 15$, $\varsigma_{1,1} = \varsigma_{2,1} = \varsigma_{3,1} = 0.8$, $\varsigma_{1,2} = \varsigma_{2,2} = \varsigma_{3,2} = 1$, $\ell_{1,1} = \ell_{2,1} = \ell_{3,1} = 0.5$, $\ell_{1,2} = \ell_{2,2} = \ell_{3,2} = 0.75$, $\vartheta_{1,1} = \vartheta_{2,1} = \vartheta_{3,1} = 1$, $\vartheta_{1,2} = \vartheta_{2,2} = \vartheta_{3,2} = 2$, $\gamma_{1,1} = \gamma_{2,1} = \gamma_{3,1} = 1.4$, $\gamma_{1,2} = \gamma_{2,2} = \gamma_{3,2} = 2$, $u_1^{\min} = u_2^{\min} = u_3^{\min} = 0.05$, $\rho_1 = 0.02$, $\rho_2 = 0.025$, and $\rho_3 = 0.015$. The simulation results are shown in Figs. 3–5. Fig. 3(a) shows that the three followers track the leader output signal with bounded consensus tracking errors. Fig. 3(b) and (c) depicts the boundedness of $\widehat{\beta}_{1,1}$, $\widehat{\beta}_{2,1}$, and $\widehat{\beta}_{3,1}$, and of $\widehat{\beta}_{1,2}$, $\widehat{\beta}_{2,2}$, and $\widehat{\beta}_{3,2}$, respectively. Fig. 4 reveals the trajectories of the actual control signals u_i and quantized control $Q_i(u_i)$, $i = 1, 2, 3$. Fig. 5 provides the evolutions of the adaptation parameters $\xi_{1,1}$, $\xi_{1,2}$, $\xi_{2,1}$, $\xi_{2,2}$, $\xi_{3,1}$, and $\xi_{3,2}$.

B. Practical Example

To further validate the developed control method, a multiagent version of the underactuated weakly coupled mechanical benchmark in [53] is considered, also shown in Fig. 6. The system includes a mass $m_{f,1}^{\sigma_f}$ on a horizontal smooth surface and an inverted pendulum $m_{f,2}^{\sigma_f}$ supported by a massless rod. The mass is connected to the wall surface by a linear spring and to the inverted pendulum by a nonlinear spring with a cubic force deformation relation. Thus, the dynamics of the fth agent can be represented by

$$\begin{cases} \ddot{\theta}_f = \dfrac{g\sin(\theta_f)}{l} + \dfrac{k_{f,s}^{\sigma_f(t)}}{m_{f,2}^{\sigma_f(t)} l}\left(x_f - l\sin(\theta_f)\right)^3\cos(\theta_f) \\ \ddot{x}_f = -\dfrac{k_{f,\omega}^{\sigma_f(t)}}{m_{f,1}^{\sigma_f(t)}}x_f - \dfrac{k_{f,s}^{\sigma_f(t)}}{m_{f,1}^{\sigma_f(t)}}\left(x_f - l\sin(\theta_f)\right)^3 + \dfrac{u_f}{m_{f,1}^{\sigma_f(t)}} \end{cases} \tag{43}$$

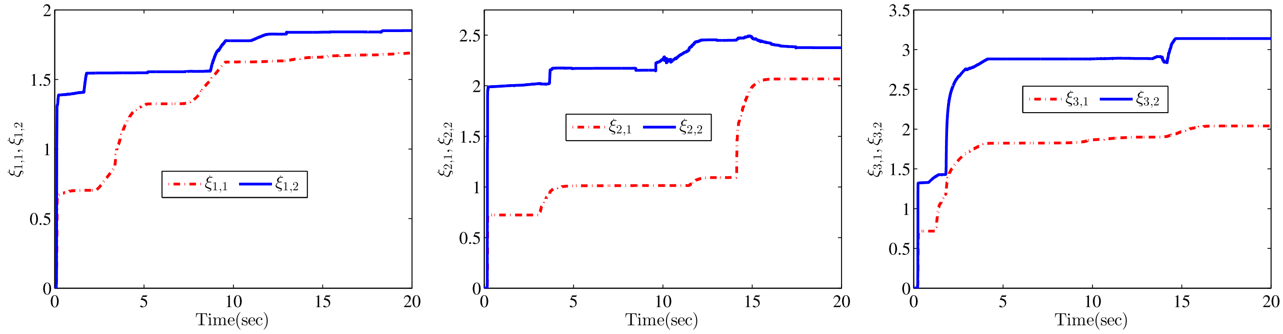

Fig. 5. Curves of $\xi_{1,1}$ and $\xi_{1,2}$, $\xi_{2,1}$ and $\xi_{2,2}$, and $\xi_{3,1}$ and $\xi_{3,2}$.

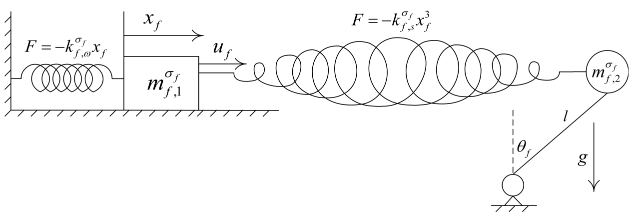

Fig. 6. Underactuated weakly coupled mechanical system.

TABLE I
PERFORMANCE INDICES FOR FOUR DIFFERENT SETS OF QUANTIZER PARAMETERS $\bar{\rho}$

Indices	$\bar{\rho}=0.02$	$\bar{\rho}=0.03$	$\bar{\rho}=0.05$	$\bar{\rho}=0.08$
ITAE	1.7281	1.5982	1.4443	1.2796
RMSE	0.2163	0.1857	0.1448	0.0958
MACA	8.6374	9.0853	10.7742	11.6563

for $f = 1, 2, 3$, and $\sigma_f(\cdot) : [0, +\infty) \to \mathcal{M}_f = \{1, 2, 3\}$, where $\theta_f \in (-[\pi/2], [\pi/2])$, x_f is the displacement of $m_{f,1}^{\sigma_f(t)}$, u_f is the control force acting on $m_{f,1}^{\sigma_f(t)}$. Moreover, $k_{f,s}^{\sigma_f(t)}$ and $k_{f,\omega}^{\sigma_f(t)}$ are spring coefficients, and l is the pendulum length. The following change of coordinates:

$$\chi_{f,1} = \theta_f, \quad \chi_{f,2} = \dot{\theta}_f, \quad \chi_{f,3} = x_{f,3}, \quad \chi_{f,4} = \dot{x}_{f,3} \tag{44}$$

transform (53) into

$$\begin{cases} \dot{\chi}_{f,1} = \chi_{f,2} \\ \dot{\chi}_{f,2} = \varphi_{f,2}^{\sigma_f(t)}(\bar{\chi}_{f,2}) + \phi_{f,2}^{\sigma_f(t)}(\bar{\chi}_{f,2})\chi_{f,3}^3 \\ \dot{\chi}_{f,3} = \chi_{f,4} \\ \dot{\chi}_{f,4} = \varphi_{f,4}^{\sigma_f(t)}(\bar{\chi}_{f,4}) + \phi_{f,4}^{\sigma_f(t)}(\bar{\chi}_{f,4})u_f \end{cases} \tag{45}$$

where $\varphi_{f,2}^{\sigma_f(t)}(\bar{\chi}_{f,2}) = (g/l)\sin(\chi_{f,1}) + ([k_{f,s}^{\sigma_f(t)}]/[m_{f,2}^{\sigma_f(t)} l])\cos(\chi_{f,1})[3\chi_{f,3} l^2 \sin^2(\chi_{f,1}) - 3\chi_{f,3}^2 l \sin(\chi_{f,1}) - l^3 \times \sin^3(\chi_{f,1})]$, $\varphi_{f,4}(\bar{\chi}_{f,4}) = -([k_{f,\omega}^{\sigma_f(t)}]/[m_{f,1}^{\sigma_f(t)}])\chi_{f,3} - ([k_{f,s}^{\sigma_f(t)}]/[m_{f,1}^{\sigma_f(t)}])[\chi_{f,3}^3 - l^3 \sin^3(\chi_{f,1}) - 3\chi_{f,3}^2 l \sin(\chi_{f,1}) + 3\chi_{f,3} l^2 \sin^2(\chi_{f,1})]$, $\phi_{f,2}^{\sigma_f(t)}(\bar{\chi}_{f,2}) = ([k_{f,s}^{\sigma_f(t)}]/[m_{f,2}^{\sigma_f(t)} l])\cos(\chi_{f,1})$, and $\phi_{f,4}^{\sigma_f(t)}(\bar{\chi}_{f,4}) = (1/[m_{f,1}^{\sigma_f(t)}])$. We take $m_{1,1}^1 = 1.25$ kg, $m_{1,1}^2 = 1.5$ kg, $m_{1,1}^3 = 1.75$ kg, $m_{1,2}^1 = 3$ kg, $m_{1,2}^2 = 2$ kg, $m_{1,2}^3 = 1.25$ kg, $m_{2,1}^1 = 1.5$ kg, $m_{2,1}^2 = 3.75$ kg, $m_{2,1}^3 = 3$ kg, $m_{2,2}^1 = 2$ kg, $m_{2,2}^2 = 2.25$ kg, $m_{2,2}^3 = 1.5$ kg, $m_{3,1}^1 = 5$ kg, $m_{3,1}^2 = 1.75$ kg, $m_{3,1}^3 = 1$ kg, $m_{3,2}^1 = 5$ kg, $m_{3,2}^2 = 1.5$ kg, $m_{3,2}^3 = 2.5$ kg; $k_{1,s}^1 = 85$ N/m^3, $k_{1,s}^2 = 70$ N/m^3, $k_{1,s}^3 = 65$ N/m^3, $k_{2,s}^1 = 95$ N/m^3, $k_{2,s}^2 = 90$ N/m^3, $k_{2,s}^3 = 75$ N/m^3, $k_{3,s}^1 = 75$ N/m^3, $k_{3,s}^2 = 98$ N/m^3, $k_{3,s}^3 = 80$ N/m^3, $k_{1,\omega}^1 = 50$ N/m, $k_{1,\omega}^2 = 45$ N/m, $k_{1,\omega}^3 = 37$ N/m, $k_{2,\omega}^1 = 50$ N/m, $k_{2,\omega}^2 = 40$ N/m, $k_{2,\omega}^3 = 45$ N/m, $k_{3,\omega}^1 = 35$ N/m, $k_{3,\omega}^2 = 55$ N/m, $k_{3,\omega}^3 = 60$ N/m, and $g = 9.8$ m/s^2.

While carrying out the simulation, the control directions of $\phi_{f,2}^{\sigma_f(t)}$, $f = 1, 2, 3$, are assumed unknown and the other control directions are assumed known. The switching signal is as in Fig. 2. Let the initial conditions be $\chi_{1,1}(0) = 5.5$, $\chi_{1,2}(0) = 0.25$, $\chi_{1,3}(0) = 0.75$, $\chi_{1,4}(0) = -0.5$, $\chi_{2,1}(0) = 3.7$, $\chi_{2,2}(0) = 0.2$, $\chi_{2,3}(0) = 0.35$, $\chi_{2,4}(0) = 0.25$, $\chi_{3,1}(0) = 1.5$, $\chi_{3,2}(0) = -0.75$, $\chi_{3,3}(0) = 0.5$, $\chi_{3,4}(0) = -0.75$, $\hat{\beta}_{1,1}(0) = 3$, $\hat{\beta}_{1,3}(0) = 1$, $\hat{\beta}_{1,4}(0) = 5$, $\hat{\beta}_{2,1}(0) = 7$, $\hat{\beta}_{2,2}(0) = 5$, $\hat{\beta}_{2,3}(0) = 3.5$, $\hat{\beta}_{2,4}(0) = 2.5$, $\hat{\beta}_{3,1}(0) = 12$, $\hat{\beta}_{3,2}(0) = 9$, $\hat{\beta}_{3,1}(0) = \hat{\beta}_{3,2}(0) = 9$, $\hat{\beta}_{3,3}(0) = \hat{\beta}_{3,4}(0) = 5.5$, and $\xi_{1,1}(0) = \xi_{1,2}(0) = \xi_{1,3}(0) = \xi_{1,4}(0) = \xi_{2,1}(0) = \xi_{2,2}(0) = \xi_{2,3}(0) = \xi_{2,4}(0) = \xi_{3,1}(0) = \xi_{3,2}(0) = \xi_{3,3}(0) = \xi_{3,4}(0) = 0$. The design parameters are chosen to be $c_{1,1} = c_{2,1} = c_{3,1} = 7.5$, $c_{1,2} = c_{2,2} = c_{3,2} = 10$, $c_{1,3} = c_{2,3} = c_{3,3} = 5$, $c_{1,4} = c_{2,4} = c_{3,4} = 5$, $\varsigma_{1,1} = \varsigma_{2,1} = \varsigma_{3,1} = 0.8$, $\varsigma_{1,2} = \varsigma_{2,2} = \varsigma_{3,2} = 1$, $\varsigma_{1,3} = \varsigma_{2,3} = \varsigma_{3,3} = 0.25$, $\varsigma_{1,4} = \varsigma_{2,4} = \varsigma_{3,4} = 1.5$, $\ell_{1,1} = \ell_{2,1} = \ell_{3,1} = 0.5$, $\ell_{1,2} = \ell_{2,2} = \ell_{3,2} = 0.75$, $\ell_{1,3} = \ell_{2,3} = \ell_{3,3} = 0.35$, $\ell_{1,4} = \ell_{2,4} = \ell_{3,4} = 0.5$, $\vartheta_{1,1} = \vartheta_{2,1} = \vartheta_{3,1} = 1$, $\vartheta_{1,2} = \vartheta_{2,2} = \vartheta_{3,2} = 2$, $\vartheta_{1,3} = \vartheta_{2,3} = \vartheta_{3,3} = 2.75$, $\vartheta_{1,4} = \vartheta_{2,4} = \vartheta_{3,4} = 1.5$, $\gamma_{1,1} = \gamma_{2,1} = \gamma_{3,1} = 1.4$, $\gamma_{1,2} = \gamma_{2,2} = \gamma_{3,2} = 2$, $\gamma_{1,3} = \gamma_{2,3} = \gamma_{3,3} = 2.5$, $\gamma_{1,4} = \gamma_{2,4} = \gamma_{3,4} = 3.5$, and $u_1^{\min} = u_2^{\min} = u_3^{\min} = 0.05$. Let $\bar{\rho} = \rho_1 = \rho_2 = \rho_3$. To investigate the effects of quantizer parameter ρ_f, $f = 1, 2, 3$, on system performances, several performance indices are used: integral time absolute error (ITAE) $[(1/3)\int_0^T t|\sum_{f=1}^3 e_{f,1}(t)|dt]$, root mean-square error (RMSE) $[(1/3T)\int_0^T |\sum_{f=1}^3 e_{f,1}^2(t)|dt]^{(1/2)}$, and mean absolute control action (MACA) $[(1/3T)\int_0^T |\sum_{f=1}^3 u_f|]$. The simulation results are given in Fig. 7 and the calculation results are summarized in Table I. It can be seen from Table I that the tracking accuracy improves as ρ_f increases, while larger control effort is required, that is, a finer quantizer leads to improved precision, which might require larger controls.

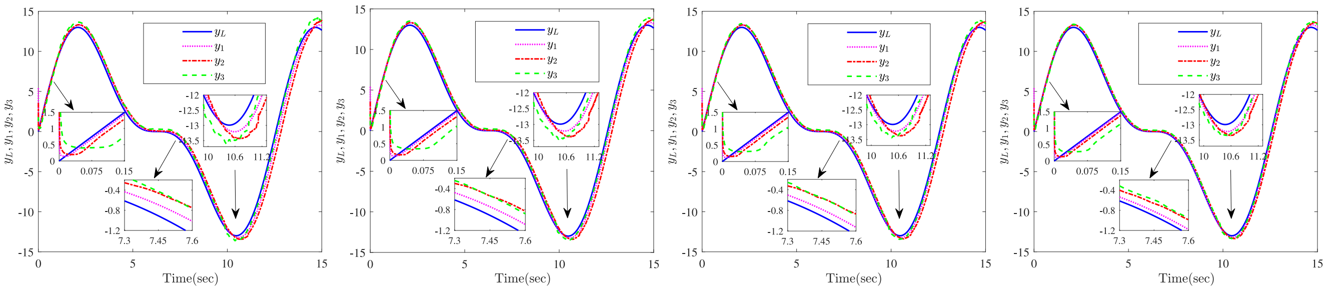

(a) (b) (c) (d)

Fig. 7. Evolutions of y_L, y_1, y_2, and y_3 under four cases: (a) $\bar{\rho} = 0{:}02$; (b) $\bar{\rho} = 0{:}03$; (c) $\bar{\rho} = 0{:}05$; and (d) $\bar{\rho} = 0{:}08$.

VI. Conclusion

This work investigated a Nussbaum function approach in the distributed adding-one-power-integrator scenario. Studying this scenario becomes necessary for classes of systems where the distributed backstepping scenario fails: this is the case of high-power dynamics, also known in the literature as high-order nonlinear dynamics. The distributed control challenges lie in the high-power nonlinear dynamics, in the switching behavior, in the input quantization and, most importantly, in the partially unknown control directions. A new lemma involving multiple Nussbaum functions and quantization decomposition parameter was constructed to handle these challenges.

Appendix A
Proof of Lemma 2

The main idea is to prove the boundedness of ξ_n on $[0, t_\nu)$ through seeking a contradiction.

For simplicity, the index f is removed in the following analysis. Without loss of generality, let us assume $\xi_1(t), \ldots, \xi_\lambda(t)$ are unbounded and $\xi_{\lambda+1}(t), \ldots, \xi_{n_f}(t)$ are bounded for $1 \leq \lambda \leq n_f$. we first rewrite (5) as

$$V(\xi_i, \xi_j) = \sum_{n=1}^{l}\left\{\int_{\xi_i}^{\xi_j} \mathcal{N}_R^{\bar{1}}(\xi_n(\nu))\theta_n\phi_n(\nu)d\xi_n(\nu)\right\} + \sum_{n=l+1}^{n_f}\left\{\int_{\xi_i}^{\xi_j} \theta_n\mathcal{N}_R^{\bar{2}}(\xi_n(\nu))\phi_n(\nu)d\xi_n(\nu)\right\} + \sum_{n=1}^{n_f}\int_{\xi_i}^{\xi_j}\iota_n d\xi_n(\nu) \tag{46}$$

where we have used the following notation for compactness: $V(\xi_i, \xi_j) = V(\xi(t_i), \xi(t_j)) = V(t_i, t_j)$. At this point, two situations should be taken into account: the first one is when $\xi_n(t)$ has no upper bound on $[0, t_\nu)$ and the second one is when $\xi_n(t)$ has no lower bound on $[0, t_\nu)$.

1) *Situation 1:* $\xi_n(t)$ has no upper bound on $[0, t_\nu)$ for $1 \leq n \leq \lambda$. Let us first consider the case $\phi_n(t) > 0$. Following the method in [45], we construct three increasing time sequences $\{t_\varrho\}$, $\{t'_\varrho\}$, and $\{t''_\varrho\}$ defined by $t_\varrho = \min_{1\leq n\leq\lambda}\{t : \xi_n(t) = (2\varrho+1)\pi\}$, $t'_\varrho = \min_{1\leq n\leq\lambda}\{t : \xi_n(t) = (2\varrho-1)\pi\}$, and $t''_\varrho = \min_{1\leq n\leq\lambda}\{t : \xi_n(t) = 2\varrho\pi\}$. It follows from the above definitions that there exists a set $\Omega_\varrho = \{\omega_\varrho\} \subset \mathcal{R}^{\omega_\varrho}$ satisfying $\xi_n(t_\varrho) = (2n+1)\pi$ for $\omega_\varrho \in [1, \lambda]$. To facilitate later analysis, we define sets $\Omega'_\varrho \subset \mathcal{R}^{\omega'_\varrho}$ and $\Omega''_\varrho \subset \mathcal{R}^{\omega_\varrho - \omega'_\varrho}$, where $\omega'_\varrho \in [0, \omega_\varrho]$. Furthermore, the bound $\xi_n(t_\varrho) \leq (2\varrho + 1)\pi$ holds if n is not from Ω_ϱ. The following steps are standard in the Nussbaum-based control literature [45] and we shall provide only the main steps for compactness. Using the above definitions, (46) can be expressed by

$$\begin{aligned} V\big(\xi_n\big(t_\varrho\big)\big) \leq{}& \sum_{n=1, n\notin\Omega_\varrho}^{\lambda}\{\int_0^{\xi_n(t_\varrho)} \phi_n(\nu)\theta_n\mathcal{N}_R(\xi_n(\nu))d\xi_n(\nu)\} \\ &+ \sum_{k=0, k\in\Omega_\varrho{'}}^{\omega'_\varrho}\left\{\int_0^{\xi_k(t_\varrho)} \phi_k(\nu)\theta_k\mathcal{N}_R^{\bar{1}}(\xi_k(\nu))d\xi_k(\nu)\right\} \\ &+ \sum_{k=0, k\in\Omega''_\varrho}^{\omega''_\varrho}\int_0^{\xi_k(t_\varrho)}\left\{\mathcal{N}_R^{\bar{2}}(\xi_k(\nu))\phi_k(\nu)\theta_k d\xi_k(\nu)\right\} \\ &+ \sum_{n=0}^{\lambda}\xi_n\big(t_\varrho\big)\iota_n + \Sigma \end{aligned} \tag{47}$$

where $\Sigma = \sum_{n=\lambda+1}^{n_f}\int_0^{\xi_n(t_\varrho)}\phi_n(\nu)\mathcal{N}_R(\xi_n(\nu))d\xi_n(\nu) + \sum_{n=\lambda+1}^{n_f}(\xi_n(t_\varrho))\iota_n$ and $\xi_n(0) = 0$. The function $V(\xi_n(t_\varrho))$ can be further bounded as

$$\begin{aligned} V\big(\xi_n\big(t_\varrho\big)\big) \leq{}& \sum_{n=1}^{\lambda}\left\{\int_0^{\xi_n\left(t'_\varrho\right)} \phi_n(\nu)\theta_n\mathcal{N}_R(\xi_n(\nu))d\xi_n(\nu)\right\} \\ &+ \sum_{n=1, k\notin\Omega_{\varrho''}}^{\lambda}\{\int_{2\varrho\pi-\pi}^{2\varrho\pi} \bar{\phi}^\star|\mathcal{N}_R^{\bar{1}}(\nu)|d\nu\} + \Sigma \\ &+ \sum_{k=1, k\in\Omega_\varrho}^{\omega_\varrho}\int_{2\varrho\pi}^{2\varrho\pi+\pi}\underline{\phi}^\star\mathcal{N}_R(\nu)d\nu + \sum_{n=0}^{\lambda}\xi_n(t_\varrho)\iota_n \end{aligned} \tag{48}$$

where $\bar{\phi}^\star = \bar{\phi}_n\bar{\theta}_n$ and $\underline{\phi}^\star = \underline{\phi}_n\underline{\theta}_n$ with $\bar{\theta}_n > 0$ and $\underline{\theta}_n > 0$ being the upper and lower bounds of θ_n for $1 \leq n \leq n_f$, respectively. Note that the integral value of $\mathcal{N}_R(\nu)$ (represented by $\mathcal{N}_T(\nu)$) on $[0, t_\nu)$ is

$$\mathcal{N}_T(\nu) = \begin{cases} -\mu\Big(1 + \exp\Big(\frac{\nu^2}{2}\Big)(\nu\sin(\nu) - \cos(\nu))\Big) \\ 1 - \exp\Big(\frac{\nu^2}{2}\Big). \end{cases} \tag{49}$$

Substituting (49) into (48) and after arrangements gives

$$\begin{aligned} V\big(\xi_n\big(t_\varrho\big)\big) =& \sum_{n=1}^{\lambda}\left\{\int_0^{\xi_n\left(t'_\varrho\right)} \phi_n(\nu)\theta_n\mathcal{N}_R(\xi_n(\nu))d\xi_n(\nu)\right\}\\ &+ (2\varrho+1)\pi\lambda\iota_{\max} - \exp\left(\frac{4\varrho^2\pi^2}{2}\right)\\ &\times\left\{\Im^\star\exp\left(\frac{(4\varrho+1)\pi^2}{2}\right)-\epsilon^\star\bar{\phi}^\star\mu\right\}\\ &- \exp\left(\frac{(2\varrho-1)^2\pi^2}{2}\right)\left\{\Im^\star\exp\left(\frac{(4\varrho-1)\pi^2}{2}\right)\right.\\ &\left.-\epsilon^\star\bar{\phi}^\star\right\}+\Sigma \end{aligned} \tag{50}$$

where $\Im^\star = \omega'_\varrho\exp(-t^\star\mu^\star)\mu + (\omega_\varrho - \omega'_\varrho)\underline{\phi}^\star\exp(-t^\star\mu^\star)$ with $t^\star = t_\varrho - t''_\varrho$, $\epsilon^\star = \lambda + \omega'_\varrho - \omega_\varrho$ and $\iota_{\max} = \max_{1\le n\le n_f}\{\iota_n\}$. Apparently, the terms on the right-hand side of (50) (except the first term) approach to negative infinity as $\varrho \to +\infty$. For the first term in (50), we define three sequences $\{t_\varrho^{2\pi}\}$, $\{t_\varrho^{4\pi}\}$, and $\{t_\varrho^{(2\varrho-4)\pi}\}$ defined by $t_\varrho^{2\pi} = \min_{1\le n\le\lambda}\{t : \xi_n(t) = 2\pi\}$, $t_\varrho^{4\pi} = \min_{1\le n\le\lambda}\{t : \xi_n(t) = 4\pi\}$, and $t_\varrho^{(2\varrho-4)\pi} = \min_{1\le n\le\lambda}\{t : \xi_n(t) = (2\varrho-4)\pi\}$. Then, it can be deduced that the value of the first term approaches to zero as $\varrho \to +\infty$. To this end, one can conclude that

$$V\big(\xi_n\big(t_\varrho\big)\big) \longrightarrow -\infty \quad \text{as} \quad \varrho \longrightarrow +\infty \tag{51}$$

which leads to a contradiction with the fact that $V(\cdot)$ is predesigned to be non-negative. As a result, $\xi_n(t)$, $1 \le n \le n_f$, are upper bounded.

2) *Situation 2:* $\xi_n(t)$ has no lower bound on $[0, t_\nu)$ for $1 \le n \le \lambda$. The proof is similar to Situation 1 and, thus, it is omitted due to space limitations.

Appendix B
Proof of Theorem 1

Consider the total Lyapunov function

$$V = \sum_{f=1}^{N} V_{f,n_f} = \sum_{f=1}^{N}\sum_{m=1}^{n_f}\left(\frac{e_{f,m}^{r_f-r_{f,m}+4}}{r_f-r_{f,m}+4} + \frac{1}{2\vartheta_{f,m}}\tilde{\beta}_{f,m}^2\right). \tag{52}$$

Applying Lemma 3 to the term $s_f^{\frac{r_{f,n}-1}{r_f+3}} e_{f,n}^{r_f-r_{f,n}+4}$ with $s_f > 0$ being a constant, the following inequality holds:

$$s_f^{\frac{r_{f,n}-1}{r_f+3}} e_{f,n}^{r_f-r_{f,n}+4} \le s_f + e_{f,n}^{r_f+3}, \quad \big(n = 1, 2, \ldots, n_f\big). \tag{53}$$

Substituting (53) into (52) and synthesizing the previous analysis, it is possible to obtain

$$\begin{aligned} V_{f,n_f}(t) \le& \sum_{n=1}^{n_f}\int_0^t \phi_{f,n}\big(\bar{\chi}_{f,n}\big)\theta_{f,n}\mathcal{N}_R\big(\xi_{f,n}\big)\dot{\xi}_{f,n}d\nu\\ &+\sum_{n=1}^{n_f}\int_0^t \dot{\xi}_{f,n}d\nu + \Pi_f \end{aligned} \tag{54}$$

where $\Pi_f = V_{f,n_f}(0) + \sum_{n=1}^{n_f}\big(s_f\big(c_{f,n} - \bar{\lambda}_{f,n}\big) + \lambda_{f,n}\big) + \sum_{n=1}^{n_f}([\gamma_{f,n}]/[2\vartheta_{f,n}])\beta_{f,n}^2$ is a positive constant.

At this point, we aim to extend the boundedness of Lemma 2 from a finite interval to the entire time domain. Along similar lines as [16], for the fth agent, we consider an augmented state vector $x_{ag} \triangleq [\chi_{f,1}, \ldots, \chi_{f,n_f}, \xi_{f,1}, \ldots, \xi_{f,n_f}, \widehat{\beta}_{f,1}, \ldots, \widehat{\beta}_{f,n_f}, \alpha_{f,1}, \ldots, u_f]^T$ so that they can describe the closed-loop dynamic system as $\dot{x}_{ag}(t) = \digamma_{ag}(t, x_{ag}(t))$ for $t \in [0, t_f)$. We start from $t = 0$; since $\digamma_{ag}(\cdot) : \mathbb{R}^+ \times \mathbb{R}^{4\times n_f} \to \mathbb{R}$ is a locally Lipschitz map with respect to $x_{ag}(t)$, a solution exists on the time interval $[0, t_\nu)$ with $t_\nu \le t_f$ (where the strict inequality holds if there is finite-time escape phenomenon [54]). It follows from (54) and Lemma 2 that $\xi_{f,n}(\cdot)$, $V_f(\cdot)$, and $\sum_{n=1}^{n_f}\int_0^t\big(\phi_{f,n}(\nu)\theta_{f,n}\mathcal{N}_R\big(\xi_{f,n}(\nu)\big) + \iota_f\big)\dot{\xi}_{f,n}(\nu)d\nu$ are bounded on the time interval $[0, t_\nu)$ for $n = 1, \ldots, n_f$, which implies $\chi_{f,1}, \ldots, \chi_{f,n_f}$, $\widehat{\beta}_{f,1}, \ldots, \widehat{\beta}_{f,n_f}$, and $\alpha_{f,1}, \ldots, u_f$ remain bounded on $[0, t_\nu)$. Hence, the whole solution x_{ag} is bounded on $[0, t_\nu)$. In accordance with [54, Ch. 8, Sec. 5], the solution of the closed-loop system $\dot{x}_{ag}(t) = \digamma_{ag}(t, x_{ag}(t))$ can be extended to t_f. Repeating the above analysis on the continuation of the solution of the closed-loop system and invoking [55, p. 476, Th. 54] we conclude that there is no finite-time escape phenomenon that will occur and the solution of the closed-loop system exists on the entire time domain $[0, \infty)$ and that $\xi_{f,n}(\cdot)$, $\widehat{\beta}_{f,n}(\cdot)$, $\alpha_{f,n}(\cdot)$, $V_f(\cdot)$, $\chi_{f,n}\cdot$ for $n = 1, \ldots, n_f$ are bounded on the entire time domain.

Let P_f be the upper bound of the integral term $\sum_{n=1}^{n_f}\int_0^t\phi_{f,n}(\bar{\chi}_{f,n})\theta_{f,n}\mathcal{N}_R\big(\xi_{f,n}\big)\dot{\xi}_{f,n}d\nu + \sum_{n=1}^{n_f}\int_0^t\dot{\xi}_{f,n}d\nu$. Considering (11) and (54), the following inequality holds:

$$\frac{e_{f,1}^{r_f-r_{f,1}+4}}{r_f-r_{f,1}+4} \le \Pi_f + P_f. \tag{55}$$

Noting (55), we know that $V_f(t) \le \Pi_f + P_f$, and the following inequality holds:

$$\big|e_{f,1}\big| \le \Upsilon_f \tag{56}$$

where $\Upsilon_f = \big(\big(\Pi_f + P_f\big)\big(r_f - r_{f,1} + 4\big)\big)^{(1/[r_f-r_{f,1}+4])}$.

From (56), we can obtain

$$\|e_1\| \le \sqrt{\sum\nolimits_{f=1}^{N}\big|e_{f,1}\big|^2} \le \sqrt{\sum\nolimits_{f=1}^{N}\Upsilon_f^2}. \tag{57}$$

Consequently, we can obtain that $\|\delta\| \le (1/[\underline{\sigma}\big(\bar{\mathcal{L}} + \mathcal{B}\big)])\sqrt{\sum_{f=1}^{N}\Upsilon_f^2}$. It is known that $\underline{\sigma}\big(\bar{\mathcal{L}} + \mathcal{B}\big)$ can be replaced by a more conservative bound $(\bar{N}/[N^2 + N - 1])$ with $\bar{N} = ([N - 1/N])^{[N-1/2]}$ [56]. This completes the proof.

References

[1] W. Ren and Y. Cao, *Distributed Coordination of Multi-Agent Networks: Emergent Problems, Models, and Issues*. London, U.K.: Springer, 2010.

[2] W. Yu, G. Wen, G. Chen, and J. Cao, *Distributed Cooperative Control of Multi-agent Systems*, 1st ed. Hoboken, NJ, USA: Wiley, 2017.

[3] W. Zhang, H. R. Karimi, and Y. Tang, "Distributed tracking for discrete-time multiagent networks via an ultrafast control protocol," *IEEE Trans. Syst., Man, Cybern., Syst.*, early access, Feb. 14, 2020, doi: 10.1109/TSMC.2020.2970212.

[4] C. L. P. Chen, G. Wen, Y. Liu, and F. Wang, "Adaptive consensus control for a class of nonlinear multiagent time-delay systems using neural networks," *IEEE Trans. Neural Netw. Learn. Syst.*, vol. 25, no. 6, pp. 1217–1226, Jun. 2014.

[5] G. Wen, C. L. P. Chen, J. Feng, and N. Zhou, "Optimized multi-agent formation control based on an identifier actor critic reinforcement learning algorithm," *IEEE Trans. Fuzzy Syst.*, vol. 26, no. 5, pp. 2719–2731, Oct. 2018.
[6] S. Ferik, A. Qureshi, and F. Lewis, "Neuro-adaptive cooperative tracking control of unknown higher-order affine nonlinear systems," *Automatica*, vol. 50, pp. 798–808, Mar. 2014.
[7] A. Das and F. Lewis, "Distributed adaptive control for synchronization of unknown nonlinear networked systems," *Automatica*, vol. 46, pp. 2014–2021, Dec. 2010.
[8] W. Wang, S. Tong, and D. Wang, "Distributed sliding-mode tracking control of second-order nonlinear multiagent systems: An event-triggered approach," *IEEE Trans. Cybern.*, vol. 49, no. 3, pp. 961–973, Mar. 2019.
[9] G. Wen, C. L. P. Chen, Y. Liu, and Z. Liu, "Neural network-based adaptive leader-following consensus control for a class of nonlinear multi-agent state-delay systems," *IEEE Trans. Cybern.*, vol. 47, no. 8, pp. 2151–2160, Aug. 2017.
[10] S. Yoo, "Distributed low-complexity fault-tolerant consensus tracking of switched nonlinear pure-feedback multi-agent systems under asynchronous switching," *Nonlinear Anal. Hybrid Syst.*, vol. 32, pp. 239–253, May 2019.
[11] M. Lv, W. Yu, J. Cao, and S. Baldi, "A separation-based methodology to consensus tracking of switched high-order nonlinear multi-agent systems," [Online]. Available: arXiv:2006.05799.
[12] S. Yoo, "Distributed consensus tracking of a class of asynchronously switched nonlinear multi-agent systems," *Automatica*, vol. 87, pp. 421–427, Jan. 2018.
[13] H. Liang, Y. Zhang, T. Huang, and H. Ma, "Prescribed performance cooperative control for multi-agent systems with input quantization," *IEEE Trans. Cybern.*, vol. 50, no. 5, pp. 1810–1819, May 2020, doi: 10.1109/TCYB.2019.2893645.
[14] Q. Wang, H. E. Psillakis, and C. Sun, "Adaptive cooperative control with guaranteed convergence in time-varying networks of nonlinear dynamical systems," *IEEE Trans. Cybern.*, early access, Jun. 3, 2019, doi: 10.1109/TCYB.2019.2916563.
[15] Q. Wang, H. E. Psillakis, and C. Sun, "Cooperative control of multiple high-order agents with nonidentical unknown control directions under fixed and time-varying topologies," *IEEE Trans. Syst., Man, Cybern., Syst.*, early access, May 27, 2019, doi: 10.1109/TSMC.2019.2916641.
[16] H. E. Psillakis, "Adaptive NN cooperative control of unknown nonlinear multiagent systems with communication delays," *IEEE Trans. Syst., Man, Cybern., Syst.*, early access, Nov. 12, 2019, doi: 10.1109/TSMC.2019.2950114.
[17] X. Li, Y. Tang, and H. R. Karimi, "Consensus of multi-agent systems via fully distributed event-triggered control," *Automatica*, vol. 116, Jun. 2020, Art. no. 108898. [Online]. Available: https://doi.org/10.1016/j.automatica.2020.108898
[18] X. Mi, Y. Zou, S. Li, and H. R. Karimi, "Self-triggered DMPC design for cooperative multiagent systems," *IEEE Trans. Ind. Electron.*, vol. 67, no. 1, pp. 512–520, Feb. 2020.
[19] M. Krstic, I. Kanellakopoulos, and P. Kokotovic, *Nonlinear and Adaptive Control Design*. New York, NY, USA: Wiley, 1995.
[20] W. Wang and S. Tong, "Adaptive fuzzy bounded control for consensus of multiple strict-feedback nonlinear systems," *IEEE Trans. Cybern.*, vol. 48, no. 2, pp. 522–531, Feb. 2018.
[21] G. Wen, X. Yu, W. Yu, and J. Lü, "Coordination and control of complex network systems with switching topologies: A survey," *IEEE Trans. Syst., Man, Cybern., Syst.*, early access, Jan. 9, 2020, doi: 10.1109/TSMC.2019.2961753.
[22] J. Long, W. Wang, J. Huang, J. Zhou, and K. Liu, "Distributed adaptive control for asymptotically consensus tracking of uncertain nonlinear systems with intermittent actuator faults and directed communication topology," *IEEE Trans. Cybern.*, early access, Sep. 26, 2019, doi: 10.1109/TCYB.2019.2940284.
[23] Y. Wang and Y. Song, "Fraction dynamic-surface-based neuroadaptive finite-time containment control of multi-agent systems in nonaffine pure-feedback form," *IEEE Trans. Neural Netw. Learn. Syst.*, vol. 28, no. 3, pp. 678–689, Mar. 2017.
[24] W. Meng, X. Liu, W. Yang, and Y. Sun, "Distributed synchronization control of nonaffine multi-agent systems with guaranteed performance," *IEEE Trans. Neural Netw. Learn. Syst.*, vol. 31, no. 5, pp. 1571–1580, May 2020, doi: 10.1109/TNNLS.2019.2920892.
[25] M. Lv, W. Yu, and S. Baldi, "The set-invariance paradigm in fuzzy adaptive DSC design of large-scale nonlinear input-constrained systems," *IEEE Trans. Syst., Man, Cybern., Syst.*. early access, Feb. 12, 2019, doi: 10.1109/TSMC.2019.2895101.
[26] S. Tong, Y. Li, and S. Sui, "Adaptive fuzzy output feedback control for switched nonstrict-feedback nonlinear systems with input nonlinearities," *IEEE Trans. Fuzzy Syst.*, vol. 24, no. 6, pp. 1426–1440, Dec. 2016.
[27] M. Lv, S. Baldi, and Z. Liu, "The non-smoothness problem in disturbance observer design: A set-invariance-based adaptive fuzzy control method," *IEEE Trans. Fuzzy Syst.*, vol. 27, no. 3, pp. 598–604, Mar. 2019.
[28] Y. Liu, L. Ma, L. Liu, S. Tong, and C. L. P. Chen, "Adaptive neural network learning controller design for a class of nonlinear systems with time-varying state constraints," *IEEE Trans. Neural Netw. Learn. Syst.*, vol. 31, no. 1, pp. 66–75, Jan. 2020.
[29] M. Lv, B. De Schutter, W. Yu, W. Zhang, and S. Baldi, "Nonlinear systems with uncertain periodically disturbed control gain functions: Adaptive fuzzy control with invariance properties," *IEEE Trans. Fuzzy Syst.*, vol. 28, no. 4, pp. 746–757, Apr. 2020.
[30] S. Yuan, B. De Schutter, and S. Baldi, "Adaptive asymptotic tracking control of uncertain time-driven switched linear systems," *IEEE Trans. Autom. Control*, vol. 62, vol. 11, pp. 5802–5807, Nov. 2017.
[31] S. Yuan, M. Lv, S. Baldi, and L. Zhang, "Lyapunov-equation-based stability analysis for switched linear systems and its application to switched adaptive control," *IEEE Trans. Autom. Control*, early access, Jun. 19, 2020, doi: 10.1109/TAC.2020.3003647.
[32] M. Lv, B. De Schutter, W. Yu, and S. Baldi, "Adaptive asymptotic tracking for a class of uncertain switched positive compartmental models with application to anesthesia," *IEEE Trans. Syst., Man, Cybern., Syst.*, early access, Oct. 17, 2019, doi: 10.1109/TSMC.2019.2945590.
[33] S. Yuan, L. Zhang, and S. Baldi, "Adaptive stabilization of impulsive switched linear time-delay systems: A piecewise dynamic gain approach," *Automatica*, vol. 103, pp. 322–329, May 2019.
[34] W. Lin and C. Qian, "Adding one power integrator: A tool for global stabilization of high-order lower triangular systems," *Syst. Control Lett.*, vol. 39, pp. 339–351, Apr. 2000.
[35] X. Zhao, X. Wang, G. Zong, and X. Zheng, "Adaptive neural tracking control for switched high-order stochastic nonlinear systems," *IEEE Trans. Cybern.*, vol. 47, no. 10, pp. 3088–3099, Oct. 2017.
[36] X. Wang, H. Li, G. Zong, and X. Zhao, "Adaptive fuzzy tracking control for a class of high-order switched uncertain nonlinear systems," *J. Franklin Inst.*, vol. 354, no. 4, pp. 6567–6587, Oct. 2017.
[37] R. D. Nussbaum, "Some remarks on a conjecture in parameter adaptive control," *Syst. Control Lett.*, vol. 3, no. 5, pp. 243–246, Jan. 1983.
[38] Z. Ding and X. Ye, "A flat-zone modification for robust adaptive control of nonlinear output feedback systems with unknown high-frequency gains," *IEEE Trans. Autom. Control*, vol. 47, no. 2, pp. 358–363, Feb. 2002.
[39] X. Ye and J. Jiang, "Adaptive nonlinear design without *a priori* knowledge of control directions," *IEEE Trans. Autom. Control*, vol. 43, no. 11, pp. 1617–1621, Nov. 1998.
[40] X. Ye, "Global adaptive control of nonlinearly parametrized systems," *IEEE Trans. Autom. Control*, vol. 48, no. 1, pp. 169–173, Jan. 2003.
[41] J. Huang, W. Wang, C. Wen, and J. Zhou, "Adaptive control of a class of strict-feedback time-varying nonlinear systems with unknown control coefficients," *Automatica*, vol. 93, pp. 98–105, Jul. 2018.
[42] Z. Chen, "Nussbaum functions in adaptive control with time-varying unknown control coefficients," *Automatica*, vol. 102, pp. 72–79, Apr. 2019.
[43] Z. Chen and J. Huang, *Stabilization and Regulation of Nonlinear Systems, A Robust and Adaptive Approach*. Heidelberg, Germany: Springer, 2015.
[44] W. Chen, X. Li, W. Ren, and C. Wen, "Adaptive consensus of multi-agent systems with unknown identical control directions based on a novel Nussbaum-type function," *IEEE Trans. Autom. Control*, vol. 59, no. 7, pp. 1887–1892, Jul. 2014.
[45] C. Chen, C. Wen, Z. Liu, K. Xie, Y. Zhang, and C. L. P. Chen, "Adaptive consensus of nonlinear multi-agent systems with non-identical partially unknown control directions and bounded modelling errors," *IEEE Trans. Autom. Control*, vol. 62, no. 9, pp. 4654–4659, Sep. 2017.
[46] K. Xie, C. Chen, F. Lewis, and S. Xie, "Adaptive compensation for nonlinear time-varying multiagent systems with actuator failures and unknown control directions," *IEEE Trans. Cybern.*, vol. 49, no. 5, pp. 1780–1790, May 2019.
[47] G. Lai, Z. Liu, C. L. P. Chen, and Y. Zhang, "Adaptive asymptotic tracking control of uncertain nonlinear system with input quantization," *Syst. Control Lett.*, vol. 96, pp. 23–29, Oct. 2016.
[48] J. Zhou, C. Wen, and G. Yang, "Adaptive backstepping stabilization of nonlinear uncertain systems with quantized input signal," *IEEE Trans. Autom. Control*, vol. 59, no. 2, pp. 460–464, Feb. 2014.

[49] W. Wang, C. Wen, and J. Huang, "Distributed adaptive asymptotically consensus tracking control of nonlinear multi-agent systems with unknown parameters and uncertain disturbances," *Automatica*, vol. 77, pp. 133–142, Mar. 2017.

[50] X. Zhao, P. Shi, X. Zheng, and J. Zhang, "Intelligent tracking control for a class of uncertain high-order nonlinear systems," *IEEE Trans. Neural Netw. Learn. Syst.*, vol. 27, no. 9, pp. 1976–1982, Sep. 2016.

[51] W. Lin and R. Pongvuthithum, "Adaptive output tracking of inherently nonlinear systems with nonlinear parameterization," *IEEE Trans. Autom. Control*, vol. 48, no. 10, pp. 1737–1745, Oct. 2003.

[52] H. E. Psillakis, "Further results on the use of nussbaum gains in adaptive neural network control," *IEEE Trans. Autom. Control*, vol. 55, no. 12, pp. 2841–2846, Dec. 2010.

[53] C. Qian and W. Lin, "Practical output tracking of nonlinear systems with uncontrollable unstable linearization," *IEEE Trans. Autom. Control*, vol. 47, no. 1, pp. 21–36, Jan. 2002.

[54] M. Hirsch and S. Smale, *Differential Equations, Dynamical Systems and Linear Algebra*. New York, NY, USA: Academic, 1973.

[55] E. D. Sontag, *Mathematical Control Theory*. London, U.K.: Springer, 1998.

[56] Y. Hong and C. Pan, "A lower bound for the smallest singular value," *Linear Algebra Appl.*, vol. 172, pp. 27–32, Jul. 1992.

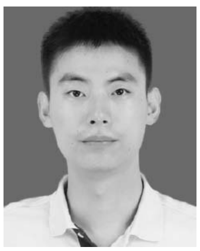

Maolong Lv received the B.Sc. degree in electrical engineering and automation and the M.Sc. degree in control science and engineering from Air Force Engineering University, Xi'an, China, in 2014, and 2016 respectively. From 2010 to 2012, he studied with Air Force Aviation University, Changchun, China. He is currently pursuing the Ph.D. degree in systems and control with the Air Force Engineering University, Xi'an, China.

He is currently affiliated with Air Force Engineering University. His research interests include nonlinear control, adaptive learning control, and swarm control and switched systems with applications in networked control, multiagent systems, and advanced fighter dynamics.

Mr. Lv was awarded a Descartes Excellence Fellowship from the Institut Français des Pays-Bas in 2018, which allowed him a research visit and a cooperation with the University of Grenoble on the topic of adaptive networked systems with emphasis on ring stability analysis for mixed traffic with human driven and autonomous vehicles from 2018 to 2019.

Wenwu Yu (Senior Member, IEEE) received the B.Sc. degree in information and computing science and the M.Sc. degree in applied mathematics from the Department of Mathematics, Southeast University, Nanjing, China, in 2004 and 2007, respectively, and the Ph.D. degree in electronic engineering from City University of Hong Kong, Hong Kong, in 2010.

He is currently the Founding Director of the Laboratory of Cooperative Control of Complex Systems and the Deputy Associate Director of the Jiangsu Provincial Key Laboratory of Networked Collective Intelligence, an Associate Director of the Research Center for Complex Systems and Network Sciences, an Associate Dean of the School of Mathematics, and a Full Professor with the Young Endowed Chair Honor, Southeast University. He held several visiting positions in Australia, China, Germany, Italy, The Netherlands, and the U.S. He publishes about 100 SCI journal papers with more than 10 000 citations. His research interests include multiagent systems, complex networks and systems, disturbance control, distributed optimization, neural networks, game theory, cyberspace security, smart grids, intelligent transportation systems, and big-data analysis.

Prof. Yu was a recipient of the Second Prize of State Natural Science Award of China in 2016. He serves as an Editorial Board Member for several flag journals, including IEEE TRANSACTIONS ON CIRCUITS AND SYSTEMS—PART II: EXPRESS BRIEFS, IEEE TRANSACTIONS ON INDUSTRIAL INFORMATICS, IEEE TRANSACTIONS ON SYSTEMS, MAN, AND CYBERNETICS: SYSTEMS, *Science China Information Sciences*, and *Science China Technological Sciences*. He was listed by Clarivate Analytics/Thomson Reuters Highly Cited Researchers in Engineering from 2014 to 2019.

Jinde Cao (Fellow, IEEE) received the B.S. degree in mathematics/applied mathematics from Anhui Normal University, Wuhu, China, in 1986, the M.S. degree in mathematics/applied mathematics from Yunnan University, Kunming, China, in 1989, and the Ph.D. degree in mathematics/applied mathematics from Sichuan University, Chengdu, China, in 1998.

He is an Endowed Chair Professor, the Dean of the School of Mathematics, the Director of the Jiangsu Provincial Key Laboratory of Networked Collective Intelligence of China, and the Director of the Research Center for Complex Systems and Network Sciences, Southeast University, Nanjing, China. He is also affiliated with Yonsei Frontier Laboratory, Yonsei University, Seoul, South Korea.

Prof. Cao was a recipient of the National Innovation Award of China, the Obada Prize, and the Highly Cited Researcher Award in Engineering, Computer Science, and Mathematics by Thomson Reuters/Clarivate Analytics. He is elected as a member of the Academy of Europe and the European Academy of Sciences and Arts, a Foreign Member of the Russian Academy of Natural Sciences, a Fellow of the Pakistan Academy of Sciences and the African Academy of Sciences, an IASCYS Academician, and a Full Member of Sigma Xi.

Simone Baldi (Senior Member, IEEE) received the B.Sc. degree in electrical engineering and the M.Sc. and Ph.D. degrees in automatic control systems engineering from the University of Florence, Florence, Italy, in 2005, 2007, and 2011, respectively.

He was a Postdoctoral Researcher with the University of Cyprus, Nicosia, Cyprus, and the Information Technologies Institute, Centre for Research and Technology Hellas, Thessaloniki, Greece. He is currently a Professor with the School of Mathematics, Southeast University, Nanjing, China, and a guest position with the Delft Center for Systems and Control, Delft University of Technology, Delft, The Netherlands, where he was an Assistant Professor. His research interests include adaptive and switched systems with applications in networked control and multiagent systems.

Prof. Baldi was awarded the outstanding reviewer of *Applied Energy* in 2016, *Automatica* in 2017, and *IET Control Theory and Applications* in 2018. Since March 2019, he has been a Subject Editor of *International Journal of Adaptive Control and Signal Processing*.